Final Technical Report

for

Aeroelastic Stability & Response of Rotating Structures

NASA Grant Number
NCC3-605

Grant Duration
November 30, 1997 to November 6, 2000

Theo G. Keith, Jr.
Principal Investigator

T.S.R. Reddy
Co-Principal Investigator

Department of Mechanical, Industrial and Manufacturing Engineering
University of Toledo
Toledo, Ohio 43606

March 2001

Aeroelastic Stability and Response of Rotating Structures

NCC3-605

Summary

A summary of the work performed under NASA grant NCC3-605 is presented. More details can be found in the cited references. This grant led to the development of relatively faster aeroelastic analyses methods for predicting flutter and forced response in fans, compressors, and turbines using computational fluid dynamic (CFD) methods.

Linearized Euler Solvers

Previous aeroelastic analyses have used the unsteady aerodynamic equations based on uniform flow. These methods neglect the effect of steady aerodynamic loading on unsteady aerodynamic forces. Steady loading is due to angle of attack and airfoil shape effects. These methods require the least amount of computational time to perform an aeroelastic analysis. Advanced methods based on computational fluid dynamic (CFD) methods have been developed to include steady loading effects in the aeroelastic analysis. However, these methods, usually based on time marching, require an enormous amount of computational time for the aeroelastic analysis.

Methods based on the linearized, unsteady, aerodynamic equations combine the benefits of the above two methods. They are faster and include steady loading effects. This is achieved by linearizing the non-linear unsteady equations using a non-linear steady aerodynamic solution to obtain linear, unsteady, aerodynamic equations. These equations can be solved in the frequency domain, by assuming harmonic motion for the unsteady oscillations. The resulting analysis code is faster and includes steady loading effects.

In this grant period, aeroelastic analysis codes have been developed using a two-dimensional (2D) linearized Euler solver, LINFLUX-2D, and a three-dimensional (3D) linearized Euler solver LINFLUX-3D. The difference between them is in using different structural models.

Also, during this grant period, a version of the LINFLUX-2D code and a version of the LINFLUX-3D code were implemented on an SGI machine, and the unsteady aerodynamic calculations were validated with published results. The execution of LINFLUX-3D required learning and running a steady aerodynamic code, TURBO-AE on SGI machines. This in turn required the development of an interface code to link the steady solution from the TURBO-AE code to the LINFLUX-3D code.

Two-Dimensional Aeroelastic Analysis code MISER-LE

A typical section structural model was used to develop the aeroelastic code, MISER-LE. The unsteady aerodynamic forces are obtained from the based on linearized Euler solver, LINFLUX-2D. This structural model has two degrees of freedom, bending and torsion. The governing aeroelastic equations are solved in the frequency domain for each interblade phase angle. Cascades with 9 and 12 blades were considered in the analysis. The unsteady aerodynamic forces were obtained from linear theory, where steady loading effects were neglected, and from LINFLUX-2D where these effects were included. The results are presented in Ref. 1. An extended version of this paper, showing an extension to forced response and correlation with previously published data is given Ref. 2.

Quasi-3D Aeroelastic Analysis code, ASTROP2-LE

In this analysis, a three-dimensional structural model is used for the aeroelastic analysis. The unsteady aerodynamic forces are obtained from LINFLUX-2D. The structural and the unsteady aerodynamic models are combined using strip theory. An existing code, ASTROP2 was taken and updated to include forced response, and the unsteady aerodynamic solution from LINFLUX-2D. The governing equations are solved in the frequency domain. The details of the resulting code ASTROP2-LE and the results for a tuned cascade aeroelastic analysis were presented in Ref. 3. The study was later extended to include mistuning effects and is being reviewed for NASA TM publication, Ref. 4.

Three-Dimensional Aeroelastic Analysis code, LINFLUX-AE

In this effort, an aeroelastic system, LINFLUX-AE, is being developed for the aeroelastic analysis of three-dimensional structures. A three-dimensional structural model was combined with the three-dimensional, unsteady, aerodynamic model LINFLUX-3D. A normal mode approach combined with the frequency domain solution method is used for aeroelastic analysis. Modules were developed to interpolate structural mode shapes on aerodynamic grids, calculation of generalized forces and flutter eigenvalues. The modules were checked with known results. The details of the preliminary version of the LINFLUX-AE code were presented in Ref. 5. The paper presents flutter calculations for a helical fan with flat plate geometry, and for a real fan, E-cubed fan. Flutter eigenvalues and work done per cycle were compared with those obtained using TURBO-AE. Further validation and extension to forced response are under progress.

References

1. Reddy, T.S.R., Srivastava, R., and Mehmed, O.: "Flutter Analysis of Cascades Using a Two Dimensional Linearized Euler solver", AIAA-98-3433, presented at the 34th Joint Propulsion Conference & Exhibit, July 13-15, Cleveland, OH.

2. Reddy, T.S.R., Srivastava, R., and Mehmed, O.: "Flutter and Forced Response Analysis of Cascades Using a Two Dimensional Linearized Euler solver", NASA TM-1999-209633, November 1999.

3. Reddy, T.S.R., Srivastava, R., and Mehmed, O.,"ASTROP2-LE: A Flutter and Forced Response Analysis System based on a Two-Dimensional Linearized Euler solver", AIAA-99-2679, presented at the 35th Joint Propulsion Conference & Exhibit, June 120-24, Los Angeles, CA.

4. Reddy, T.S.R., Srivastava, R.: and Mehmed, O.:"ASTROP2-LE: A Mistuned Aeroelastic Analysis System based on a Two-Dimensional Linearized Euler solver", to be published as NASA TM.

5. Reddy, T.S.R., Bakhle, M.A., Keith, Jr., T.G., and Mehmed, O.: "Development of a Turbomachinery Aeroelastic Code Based on a 3D Linearized Euler Solver", AIAA-2000-3230, presented at the 36th Joint Propulsion Conference & Exhibit, July 17-19, Huntsville, Al

AIAA-98-3433

Flutter Analysis of Cascades Using a Two Dimensional Linearized Euler Solver

T. S. R. Reddy
R. Srivastava

University of Toledo
Toledo, Ohio

O. Mehmed

NASA Lewis Research Center
Cleveland, Ohio

34th AIAA/ASME/SAE/ASEE
Joint Propulsion Conference & Exhibit
July 13-15, 1998 / Cleveland, OH

FLUTTER ANALYSIS OF CASCADES USING A TWO DIMENSIONAL LINEARIZED EULER SOLVER

T. S. R. Reddy *, **R. Srivastava** *
The University of Toledo
Toledo, Ohio 43606

Oral Mehmed †
NASA Lewis Research Center
Cleveland, Ohio 44135

ABSTRACT

Flutter analysis is presented for a cascade of blades in subsonic and transonic flow. The structural model for each blade is a typical section with bending and torsion degrees of freedom. The unsteady aerodynamic forces are obtained by solving unsteady linearized Euler equations. The unsteady linearized equations are obtained by linearizing the unsteady non-linear equations about the steady flow. The predicted unsteady aerodynamic forces include the effect of steady aerodynamic loading due to airfoil shape, thickness and angle of attack. The unsteady aerodynamic and aeroelastic equations are solved in the frequency domain. The present aeroelastic solver showed good correlation with published results. Further improvements are required to use the unsteady aerodynamic model in a design cycle.

INTRODUCTION

The aeroelastic research program at NASA Lewis Research Center is focused on flutter (unstalled, stalled, and whirl), and forced response analysis of propulsion components. An overview of this research was presented in Ref. 1. The review showed that a range of aerodynamic and structural models have been used to obtain the aeroelastic equations. Both, time and frequency domain methods have been used to obtain unsteady aerodynamic forces and to solve the aeroelastic equations. It was noted that time domain methods require large computational time compared to frequency domain methods, and should only be used when non-linearities are expected, and may be used in the final design.

Two approaches have been used in obtaining the unsteady aerodynamic forces using frequency domain methods. In the first approach, Refs. 2-6, the unsteady aerodynamic equations are linearized about a uniform flow, there by neglecting the effects of airfoil shape, thickness, and angle of attack. The unsteady aerodynamic models developed in Refs. 3-6 have been used to study the flutter and forced response analysis of a compressor cascade using a typical section structural model, in Refs. 7-8. However, methods developed by this approach are restricted to shock-free flows through lightly-loaded blade rows. In the second approach, Ref. 9, the unsteady flow is regarded as a small amplitude perturbation about a non-uniform steady flow. The unsteady non-linear aerodynamic equations are linearized about the non-uniform steady flow, resulting in variable coefficient linear unsteady aerodynamic equations, which include the effects of steady aerodynamic loading due to airfoil shape, thickness and angle of attack.

Following the second approach, Refs. 10-11 developed a nonlinear steady and linear unsteady aerodynamic model based on the potential equation. This unsteady aerodynamic model was used to study the effect of steady aerodynamic loading on flutter stability using a typical section structural model in Ref. 12. However, the formulation based on the potential equation requires corrections for entropy and flow rotation. The Euler equations can be used to correctly model rotational and entropy effects associated with strong shocks. Unsteady linearized Euler aerodynamic models that include the effect of steady aerodynamic loading were developed in Refs. 13-15.

Recently, a two dimensional linearized Euler code named LINFLX2D was developed in Ref. 16 under a NASA contract. This code is based on the non-linear Euler solver, NPHASE, developed in Ref.

---

* Senior Research Associate, Member AIAA
† Research Engineer, Member AIAA

17. The objectives of the present study are (1) to couple the LINFLX2D code with the aeroelastic code MISER (Refs. 7,8), (2) validate the aeroelastic predictions, and (3) evaluate LINFLX2D code for its usefulness in a aeroelastic design cycle. The MISER code at present calculates the aeroelastic stability using the unsteady aerodynamic models based on classical linear theories (theories based on flat plate geometry formulation). MISER code is selected because the typical section structural model with pitching and plunging degrees of freedom is the basis for aeroelastic formulation. This is in line with the unsteady aerodynamic model of LINFLX2D. In the present paper flutter analysis of a cascade of blades is presented using the frequency domain approach for a two dimensional cascade model. Two degrees of freedom, plunging and pitching, are considered in the analysis. Brief descriptions of the formulation and method of analysis are given in the next section, followed by results and discussion.

FORMULATION

The aerodynamic model and the aeroelastic formulation are described in this section.

Aerodynamic model

Non-linear Steady Euler Solver, NPHASE

The steady aerodynamic model is based on the unsteady, two dimensional, Euler equations. The equations in conservative differential form are solved in a time dependent body-fitted curvilinear reference frame. This transformation process and the ensuing numerical method are presented in detail in Ref. 17. The equations are discretized and solved using a finite volume method using a TVD scheme. The steady solutions presented herein are obtained using the basic implicit scheme developed in Ref. 17, which is third order accurate spatially and second order accurate in time.

Linear Unsteady Euler Solver, LINFLX2D

To obtain the linearized unsteady Euler equations, Ref. 16, the independent variables in the unsteady non-linear Euler equations are expanded in an asymptotic series of the form

$$U = U(x) + u(x(x,t),t) + \text{ higher order terms} \quad (1)$$

Assuming the unsteady excitations are harmonic in time, and with the first order variable to be represented as complex valued, the above equation can be written as

$$U = U(x) + \mathrm{Re}[u(x)\exp(iwt)] + \text{higher order terms} \quad (2)$$

Here, the term U(x) is of order one and the second term is of the order e.

Substituting the expansion of Eqs. 1 and 2 in the nonlinear unsteady Euler equations, and equating terms of like power in e, and neglecting terms of second and higher order in e, nonlinear steady equations and linear variable coefficient unsteady equations are obtained.

For harmonic blade motions with constant phase angle between adjacent blades (interblade phase angle), the values of interblade phase angle (s) that can occur are given as (Ref. 18).

$$\sigma_r = 2\pi r / N \qquad r = 0, 1, 2, \cdots, N-1 \quad (3)$$

N is the number of blades in the cascade. In a time domain approach, the number of blocks required depends on the inter blade phase angle, and small phase angles may require large number of blocks to calculate the unsteady aerodynamic forces. However, with the linear approach, the periodic conditions are applied on a single extended blade passage region i.e. a region of angular pitch,

$$\theta = 2^* \pi / N \quad (4)$$

In solving the linear unsteady equations, the independent variables are regarded as pseudo time dependent. This allows solutions to be determined using conventional time -marching algorithms to converge the steady and the complex amplitudes of the unsteady conservation variables to their steady state values. For more details, see reference 16.

Grid and Boundary Conditions

The flow equations are solved on a passage-centered H-grid. Two grid blocks are shown in Fig. 2 for calrity. Within a typical grid block, the lower computational boundary contains the upper surface of one blade in the cascade, while the upper computational boundary contains the lower

surface of the adjacent blade. Periodic boundaries in the blade-to-blade direction extend upstream and downstream from the blade surfaces. The inlet boundary corresponds to the left computational boundary and the outflow corresponds to the right boundary. The airfoil upper and lower surfaces are located along lines B-C and F-G, respectively where solid wall boundary conditions are employed. Lines A-E and D-H represent inflow and outflow boundaries, respectively. For subsonic flow these conditions are set using characteristic variable boundary conditions. The procedure used is to fix the incoming flow incidence angle and adjust the back pressure (uniform across D-H) until the average Mach number along the inflow boundary (A-E) matches some specified value. For supersonic flow, the inlet conditions are assumed to be uniform by specifying the flow density, velocity, flow angle, and pressure. The outflow variables are extrapolated from the interior by using simple first-order model. Periodicity is imposed between lines A-B and E-F, and lines C-D and G-H.

Aeroelastic model

For completeness, the aeroelastic formulation in the frequency domain (Refs. 7,8) is presented in this section. The analysis is presented for a generally mistuned cascade in which each blade may have different structural properties. The analysis for the special case of a tuned cascade in which all blades are identical is presented in the subsequent section. The approach followed assumes that the structure is vibrating in an aeroelastic mode (interblade phase angle mode) with a motion that is a harmonic function of time. The frequency of oscillation is permitted to take on complex values thus allowing decaying-, growing- or constant-amplitude oscillations. The aerodynamic forces corresponding to constant-amplitude harmonic oscillations are inserted into the equations of motion to formulate a complex eigenvalue problem. The eigenvalues are generally complex quantities, and therefore a complex frequency is obtained. The real part of the complex frequency represents the damping ratio and thus its sign determines whether the motion is decaying or growing; the imaginary part represents the damped frequency of oscillation.

Aeroelastic analysis for mistuned cascades

The equations of motion for the typical section (see Fig. 1) with structural damping can be written in matrix form for the s^{th} blade as:

$$[M_s]\{\ddot{q}_s\} + [C_s]\{\dot{q}_s\} + [K_s]\{q_s\} = \{f_s\} = \{f_{as}^{q}\} + \{f_{as}\} \quad (5)$$

where $\{f_a{}^q\}$ denotes motion-dependent aerodynamic loads and $\{f_a\}$ denotes motion-independent aerodynamic loads.

For the two degrees of freedom considered here, equation 5 can be rewritten as

$$\begin{bmatrix} 1 & x_{\alpha s} \\ x_{\alpha s} & r_{\alpha s}^2 \end{bmatrix} \begin{Bmatrix} \ddot{h}_s/b \\ \ddot{\alpha}_s \end{Bmatrix} + \begin{bmatrix} 2\omega_{hs}\zeta_{hs} & 0 \\ 0 & 2r_{\alpha s}^2\omega_{\alpha s}\zeta_{\alpha s} \end{bmatrix} \begin{Bmatrix} \dot{h}_s/b \\ \dot{\alpha}_s \end{Bmatrix} + \begin{bmatrix} \omega_{hs}^2 & 0 \\ 0 & r_{\alpha s}^2\omega_{\alpha s}^2 \end{bmatrix} \begin{Bmatrix} h_s/b \\ \alpha_s \end{Bmatrix} = \begin{Bmatrix} f_{hs}/m_s b \\ f_{\alpha s}/m_s b^2 \end{Bmatrix} \quad (6)$$

where h is the plunging (bending) displacement normal to the chord, α is the pitching (torsion) displacement, x_α the distance between the elastic axis and center of mass in semi-chord units; r_α is the radius of gyration about the elastic axis in semi-chord units; ζ_h and ζ_α are the damping ratios; b is the airfoil semi-chord; ω_h is the uncoupled natural frequency for bending; ω_α is the uncoupled natural frequency for torsion; f_h and f_α are the aerodynamic loads and s varies between 0 and N-1.

It is assumed that the motion of the blades is harmonic in time with a frequency ω and is given by

$$\begin{Bmatrix} h_s/b \\ \alpha_s \end{Bmatrix} = \begin{Bmatrix} h_{os}/b \\ \alpha_{os} \end{Bmatrix} e^{i\omega t} = \sum_{r=0}^{N-1} \begin{Bmatrix} h_{ar}/b \\ \alpha_{ar} \end{Bmatrix} e^{i\omega t} e^{i\sigma_r s} \quad (7)$$

Note that the motion has been represented as the sum of contributions from each interblade phase angle mode in which each blade has an amplitude h_{ar}/b, α_{ar} and the phase angle between adjacent blades is given by Eq. 3.

The corresponding aerodynamic forces can be written in terms of the complex-valued unsteady aerodynamic coefficients l_{hh} , $l_{\alpha h}$, $l_{h\alpha}$, $l_{\alpha\alpha}$, l_{wh}, and $l_{w\alpha}$.

$$\begin{Bmatrix} f_{hs}/m_s b \\ f_{\alpha s}/m_s b \end{Bmatrix} = \frac{\omega}{\mu_s} \sum_{r=0}^{2N-1} \begin{bmatrix} l_{hhr} h_{ar}/b + l_{h\alpha r}\, \alpha_{ar} \\ l_{\alpha hr} h_{ar}/b + l_{\alpha\alpha r}\, \alpha_{ar} \end{bmatrix} e^{i\omega t} e^{i\sigma_r s} + \frac{\omega}{\mu_s} \sum_{r=0}^{2N-1} \begin{Bmatrix} l_{whr} \\ l_{w\alpha r} \end{Bmatrix} e^{i\omega t} e^{i\sigma_r s}$$

(8)

where $\mu_s = m_s / \pi\rho_\infty b^2$ is the mass ratio of the blade.

Using Eq. 7 and Eq. 8, Eq. 6 can be written as

$$-[M_s]\begin{Bmatrix} h_{os}/b \\ \alpha_{os} \end{Bmatrix} e^{i\omega t} + \lambda\,[K_s]\begin{Bmatrix} h_{os}/b \\ \alpha_{os} \end{Bmatrix} e^{i\omega t}$$

$$= \sum_{r=0}^{N-1} [A_r]\begin{Bmatrix} h_{ar}/b \\ \alpha_{ar} \end{Bmatrix} e^{i\sigma_r s} e^{i\omega t} + \sum_{r=0}^{N-1} \{AD_r\} e^{i\sigma_r s} e^{i\omega t} \qquad (9)$$

where

$$[M_s] = \mu_s \begin{bmatrix} 1 & x_\alpha \\ x_\alpha & r_\alpha^2 \end{bmatrix}$$

$$[K_s] = \begin{bmatrix} (\omega_{hs}/\omega_o)^2 (1+2i\zeta_{hs}) & 0 \\ 0 & r_{\alpha s}^2 (\omega_{\alpha s}/\omega_o)^2 (1+2i\zeta_{\alpha s}) \end{bmatrix}$$

$$[A_r] = \begin{bmatrix} l_{hhr} & l_{h\alpha r} \\ l_{\alpha hr} & l_{\alpha\alpha r} \end{bmatrix}$$

$$\{AD_r\} = \begin{Bmatrix} l_{whr} \\ l_{w\alpha r} \end{Bmatrix} \qquad \lambda = (\omega_o/\omega)^2$$

ω_O = reference frequency and the damping terms are approximated as,

$$2i\omega\omega_{hs}\zeta_{hs} \approx 2i\omega_{hs}^2\,\zeta_{hs}$$
$$2ir_{\alpha s}^2\omega\omega_{\alpha s}\zeta_{\alpha s} \approx 2ir_{\alpha s}^2\,\omega_{\alpha s}^2\zeta_{\alpha s} \qquad (10)$$

To proceed further, the equations for all the *N* blades on the disk must be considered. For the assumed harmonic blade motion, the displacements {X} of all blades can be written as a sum of contributions from all interblade phase angles as

$$\{X\}e^{i\omega t} = [E]\{Y\}e^{i\omega t} \qquad (11)$$

where {Y} consists of the displacement amplitudes corresponding to the rth interblade phase angle and [E] is the transfer matrix, the elements of which are given by

$$E(s,r) = e^{2\pi sri\ /N}$$

where s is the blade counter and r is the interblade phase angle counter.

Using this relation, we obtain:

$$-[E]^{-1}[M][E]\{Y\} + \lambda\,[E]^{-1}[K][E]\{Y\} = [A]\{Y\} + \{AD\} \qquad (12)$$

where

[M] is the mass matrix for all blades with diagonal elements consisting of mass matrix of each blade. Similarly [K] is the stiffness matrix and [A] is the aerodynamic matrix for all blades, {AD} is the aerodynamic forces due to wake on all the blades.

Finally, after rearranging, the equations can be written as:

$$\left[[P] - \lambda\,[Q]\right]\{Y\} = -\{AD\} \qquad (13)$$

where

$$[P] = \left[[E]^{-1}[M][E] + [A]\right]$$

$$[Q] = [E]^{-1}[K][E]$$

For a stability calculation (flutter), the motion-independent forces {AD} are set to zero and the eigenvalue problem is obtained in the standard form:

$$\left[[P] - \lambda\,[Q]\right]\{Y\} = \{0\} \qquad (14)$$

The solution of the above eigenvalue problem (14) results in 2*N* complex eigenvalues of the form

$$i\,\frac{\omega}{\omega_o} = \frac{i}{\sqrt{\lambda}} = \bar{\mu} + i\,\bar{\nu} \qquad (15)$$

The real part of the eigenvalue ($\bar{\mu}$) represents the damping ratio, and the imaginary part ($\bar{\nu}$) represents the damped frequency; flutter occurs if $\bar{\mu} \geq 0$ for any of the eigenvalues.

The aeroelastic response of the blades induced by wakes is calculated from equation (13) as

$$\{Y\} = -\left[[P] - \lambda\,[Q]\right]^{-1}\{AD\} \qquad (16)$$

The amplitude of each blade is obtained by substituting equation (16) into equation (11).

Aeroelastic analysis for a tuned cascade

For a tuned cascade (or rotor), in which all the blades are identical, the foregoing analysis can be simplified considerably. In this case, the aeroelastic modes consist of individual blades vibrating with equal amplitudes with a fixed interblade phase angle between adjacent blades. Hence, for this problem, the motion of the typical blade is written as

$$\begin{Bmatrix} h_s/b \\ \alpha_s \end{Bmatrix} = \begin{Bmatrix} h_{os}/b \\ \alpha_{os} \end{Bmatrix} e^{i\omega t} = \begin{Bmatrix} h_{ar}/b \\ \alpha_{ar} \end{Bmatrix} e^{i\omega t} e^{i\sigma_r s} \qquad (18)$$

Thus the equation for the blade becomes

$$-[M_s]\begin{Bmatrix} h_{ar}/b \\ \alpha_{ar} \end{Bmatrix} e^{i(\omega t+\sigma_r s)} + \lambda\,[K_s]\begin{Bmatrix} h_{ar}/b \\ \alpha_{ar} \end{Bmatrix} e^{i(\omega t+\sigma_r s)} = [A_r]\begin{Bmatrix} h_{ar}/b \\ \alpha_{ar} \end{Bmatrix} e^{i(\omega t+\sigma_r s)} + \{AD_r\} e^{i(\omega t+\sigma_r s)} \qquad (19)$$

Since the blades are identical, the same equation is obtained for each blade. Thus, no additional information can be obtained by assembling the equations for all the blades on the disk as was done for the general mistuned system. Instead, equation (19) is solved for *N* different values of the interblade phase angle given by equation (3). As before, the equations for the forced-response problem are obtained by setting the motion-dependent forces to zero; the equations for the flutter problem are obtained by setting the motion-independent forces to zero.

For the stability calculation, the equation can be simplified as

$$\left[[P_r] - \lambda\,[I]\right]\{Y\} = \{0\} \qquad (20)$$

where

$$[P_r] = \begin{bmatrix} \dfrac{\mu + l_{hhr}}{\mu\,(\omega_h/\omega_\alpha)^2\,(1+2i\zeta_h)} & \dfrac{\mu x_\alpha + l_{h\alpha r}}{\mu\,(\omega_h/\omega_\alpha)^2\,(1+2i\zeta_h)} \\ \dfrac{\mu x_\alpha + l_{\alpha hr}}{\mu\, r_\alpha^2\,(1+2i\zeta_\alpha)} & \dfrac{\mu r_\alpha^2 + l_{\alpha\alpha r}}{\mu\, r_\alpha^2\,(1+2i\zeta_\alpha)} \end{bmatrix}$$

where the subscript *'s'* identifying the blade has been dropped and the reference frequency ω_o has been chosen to be equal to the torsional frequency ω_α.

The solution of the above eigenvalue problem results in two complex eigenvalues of the form $\bar{\mu} + i\,\bar{\nu}$, and flutter occurs if $\bar{\mu} \geq 0$. For the tuned cascade, the stability of each phase angle mode is examined separately. Hence, the interblade phase angle is fixed at one of the values given by equation (3), and the 2X2 eigenvalue problem is solved. The value of interblade phase angle is then changed, and the procedure is repeated for each of the *N* permissible values. The critical phase angle is identified as the one which results in the lowest flutter speed.

Stability calculation

The aerodynamic coefficients are calculated before the eigenvalue problem can be set up and solved. Since the unsteady aerodynamic coefficients depend on the frequency of oscillation, it is necessary to assume a frequency ω (reduced frequency of blade vibration based on chord, k_C) in advance to be able to calculate the aerodynamic coefficients. In actual calculations, the aerodynamic coefficients are functions of inlet Mach number M_∞, and interblade phase angle σ_r, in addition to cascade geometric parameters. In the present study, for a given inlet Mach number, and the reduced frequency is varied until the real part of one of the eigenvalues $\bar{\mu}$ becomes zero while the real parts of the remaining eigenvalues are negative. The assumed flutter-reduced frequency k_{cf} and the calculated flutter frequency $\bar{\nu}_f$ are both based on ω_f. Thus, these two can be combined to eliminate ω_f and the flutter speed is obtained, namely, $V_f = \bar{\nu}_f\, c\, \omega_o / k_{cf}$. Since the inlet Mach

number is known, this flutter speed gives the inlet condition (speed of sound, a_∞) at which the cascade will be neutrally stable for the given Mach number. This procedure can be repeated to obtain a plot of flutter speed versus Mach number. Knowing the operating conditions, it is possible to determine whether flutter will occur within the operating region and if so, the Mach number and frequency at flutter. It should be noted that the analysis of a mistuned cascade requires the solution of the equations for all phase angles at one time for a given reduced frequency.

RESULTS AND DISCUSSION

The analysis methods presented earlier are now applied to investigate the behavior of cascades oscillating in pitch and plunge. First, unsteady pressure distributions and loading for selected cascade configurations are presented and compared with published results to help validate the present linearized unsteady Euler solver. Finally, flutter predictions with and without mistuning are presented. For the calculation of unsteady aerodynamic coefficients, first NPHASE, the non-linear Euler solver is used to generate the steady solution. This steady solution is then used as an input to the LINFLX2D to calculate the unsteady aerodynamic forces due to small unsteady perturbations in pitch and plunge.

Code Validation

Calculations were made for a flat plate cascade, and a cascade comprising of airfoils designated as the tenth standard configuration (C10), Ref. 16. Both the cascades have a stagger angle of 45 degrees, and a gap to chord ratio (s/c) of unity. The tenth standard configuration airfoils are constructed by superposing the thickness distribution of a modified NACA 5506 airfoil on a circular-arc camber line. See Ref. 16 for more details. Two Mach numbers are considered, M=0.7 and M=0.8 for a reduced frequency of oscillation based on semichord (k_b) of 0.5. For M=0.8, the flow is transonic with a shock at 25% chord from the leading edge of the airfoil. The steady angle of attack is zero for the flat plate geometry, and ten degrees for the C10 airfoil for subsonic flow (M=0.7), and thirteen degrees for transonic flow (M=0.8). A H-grid of 141x41 grid is used for the study. There are 80 points on the airfoil, and the inlet boundary is 5 chords from the airfoil leading edge and the exit boundary is 10 chords from the airfoil trailing edge. Some calculations were also done with a 151x41 grid for which the inlet and exit boundaries are located at one chord from the leading and trailing edges respectively. There are 55 points on the airfoil for this grid.

Unsteady Aerodynamic Pressures

Subsonic Inflow

Figure 3a shows the unsteady pressure difference distribution obtained for the flat plate geometry operating at M=0.7. The interblade phase angle, σ, is 180 degrees, the reduced frequency of oscillation based on semichord is 0.5, and the Mach number of 0.7. The blades are oscillating in pitch about the midchord. For the inlet Mach number of 0.7, the flow is shock free. Figure 3a shows predictions form linear theory (Ref. 3) and from the present linearized Euler code, LINFLX2D. The predictions from LINFLX2D correlate well with the linear theory results.

Figure 3b shows the unsteady pressure distribution obtained for the standard cascade configuration, C10. The flow to the cascade is at 10 degrees angle of attack. Again, the interblade phase angle is 180 degrees, the reduced frequency of oscillation based on semichord is 0.5, and the Mach number of 0.7. The blades are oscillating in pitch about the midchord. For the inlet Mach number of 0.7, the flow is shock free. Figure 3b shows predictions form linear theory (Ref. 3), nonlinear Euler (Ref. 17) and from the present linearized Euler code, LINFLX2D. The predictions from LINFLX2D correlate well with the nonlinear Euler results. As expected, they show discrepancy with linear theory since the effects of airfoil geometry, and angle of attack are not included in the linear theory.

Transonic Inflow

For the standard configuration, C10, and for an inlet Mach number of 0.8, the flow is transonic with a normal shock occurring in each blade passage. The steady angle of attack is 13 degrees. The steady Mach number distribution for this flow obtained from NPHASE is shown in Fig. 4a which shows a normal shock at about 28% of the chord. Results from the full potential solver, Ref. 19, are also included for comparison. Both results agree well, except that the nonlinear steady Euler solver, NPHASE, predicts the shock location slightly downstream of that predicted by the full potential

solver of Ref. 19. A shock fitting procedure was used in Ref. 19, whereas the shock is captured naturally in the present solver. The unsteady pressure distribution is shown in Fig. 4b, along with a comparison with linear theory (Ref. 3) and from the unsteady nonlinear Euler solver. The unsteady results are for pitching about mid-chord with $k_b = 0.5$, $\sigma = 180°$ and amplitude of oscillation, α_0 ,= 2°. As expected, linear theory does not show any shock, indicating that unsteady analysis based on linear theory will not be accurate for cascade flutter analysis in transonic flow.

Similar results were obtained for plunging motion for both subsonic and transonic inflows.

Unsteady Aerodynamic Force coefficients

It is the unsteady aerodynamic force coefficients, unsteady lift and moment that are obtained by integrating unsteady pressure differences, that are used in the flutter and forced response prediction. Table 1 shows the unsteady aerodynamic force coefficients obtained using the Smith code, Ref. 3, and the present LINFLX2D code. Calculations were also done with the non-linear Euler solver of Ref. 19. In table 1, the first column shows the geometry of the airfoil studied, the fourth and fifth columns show the force components for pitching motion and plunging motion respectively. The symbols in the second column are *cl* for lift coefficient, and *cm* for moment coefficient, with moment taken about the mid chord (x0=0.5). The first row shows the calculations for the flat plate geometry in subsonic flow, the second row for the airfoil in subsonic flow, and the third row for the airfoil in transonic flow. The notation indicating the analysis method is given at the bottom of the table. The geometry and unsteady conditions are given on the top of the table.

A comparison of the force coefficients for flat plate geometry in the first row shows that the prediction by LINFLX2D are very close to those given by Smith code. For a flat plate geometry in subsonic flow, the Smith code gives the exact answer. It is to be noted that the flat plate is unloaded and shock free. The values of the force coefficients in the second row show some difference from the Smith code, since in LINFLX2D the effect of airfoil and angle of attack are included. The force coefficients in the third row include the effect of shock and its motion in addition to the effects of airfoil shape and angle of attack. The force coefficients obtained with LINFLX2D code compare well with those obtained from a non-linear unsteady Euler solution, indicating that LINFLX2D code can be used to analyze cascades in transonic flow. It is to be noted that with 151x41 grid, solutions for transonic flow could not be obtained with LINFLX2D code. It was suggested that for the LINFLX2D code to work properly, it is better if the inlet and exit boundaries are at least 5 chords from the leading and trailing edges respectively (Ref. 20).

Flutter Calculations

As mentioned before, given the unsteady aerodynamic force coefficients, the MISER code calculates the aeroelastic stability of tuned and mistuned cascades oscillating in pitch and plunge. The aeroelastic stability results from MISER are presented as a root locus plot, with real part of the eigenvalue indicating damping and the imaginary value indicating frequency for all possible interblade phase angles. In the present study LINFLX2D is loosely coupled with MISER (Ref. 7) to calculate flutter of mistuned cascades. First a steady solution is obtained from NPHASE for the required cascade geometry and flow conditions. With the steady solution as input, LINFLX2D is run for given a reduced frequency, interblade phase angle, and mode of interest (pitching or plunging). The unsteady aerodynamic coefficients obtained from LINFLX2D are then stored in a data base, and later used in MISER to calculate the stability characteristics.

The structural properties are the mass ratio, m, is 258.50, ratio of bending to torsion frequencies w_h /w_a is 0.357, the radius of gyration about the elastic axis in semi-chord units, r_a ,is 0.5774, with no structural damping. The elastic axis is at midchord i.e. ah = 0.0. The distance between the elastic axis and center gravity, x_a, is zero, indicating that coupling between bending and torsion is very weak and the flutter mode is dominated by torsional motion. Therefore, only torsion mode is shown for all the calculations. It should be noted that these structural properties were also used in Refs. 7 and 8.

The following procedure is used for stability prediction: First MISER is run for the selected cascade (rotor) using linear theory to identify the flutter point. Then MISER is run in conjunction with LINFLX2D data base for this flutter condition, and the eigenvalues obtained from linear theory and LINFLX2D are compared.

Flat Plate Cascade

To validate the coupling of the unsteady

aerodynamic coefficients obtained from LINFLX2D with MISER, a nine bladed cascade with a flat plate geometry was selected. The flutter results obtained are compared with those obtained from linear theory. The gap to chord ratio is unity and the stagger angle is 45 degrees. For the nine bladed cascade, for a given reduced frequency, the unsteady force coefficients have to be calculated for the possible interblade phase angles of 0.0, 40.0, 80.0, 120.0, 160.0, 200.0, 240.0, 280.0, and 320.0 degrees.

Using linear theory, for M=0.7 with elastic axis at midchord, for the nine bladed cascade mentioned above, the instability was observed to occur at k_b = 0.18 and for a phase angle of 80 degrees. Therefore, LINFLX2D is run for this value of reduced frequency, but for all allowable phase angles, and for both plunging and pitching oscillations, and a database is prepared. Then MISER is run to predict stability boundary with the unsteady aerodynamic force coefficient data base obtained from LINFLX2D.

The root locus plot showing the real and imaginary parts of the eigenvalues for the flat plate geometry obtained for torsion motion is given in Fig.5. The unsteady force coefficients for eight phase angles were obtained with LINFLX2D. For the σ =40 degrees, for which acoustic resonance was expected, the LINFLX2D code did not give a solution for the grid, oscillation of amplitude, and time step considered. This case will be studied further in future. It was noted that for a flat plate geometry, the computational times were higher than those for airfoil geometry (presented below). Figure 5 shows the comparison between predictions from linear theory and from LINFLX2D. It can be seen from Fig. 5 that LINFLX2D compares very well with linear theory results for the flat plate geometry. The plot shows that the cascade is unstable for the properties considered.

Mistuned Cascade

Results are presented now for cascades with mistuning. The type of mistuning considered is the one in which the odd and even numbered blades have different torsional frequencies, also known as alternate blade mistuning. This has been studied in Refs. 7 and 8 with 1% and 1.5% alternate mistuning. It is to be noted that in the case of 1% mistuning, the frequency ratio ω_α / ω_0 is 1.005 for all the even blades, and is 0.995 for all the odd blades. The study in Ref. 7 and 8 considered a 56 bladed cascade, and showed that alternate mistuning has a considerable effect on stability. A 12 bladed cascade is considered for the present study, to limit the computational time. MISER was run first for this case as a tuned cascade with linear theory, for M=0.7. It was found that the cascade is unstable for k_b = 0.1 and σ = 60°. This value of k_b = 0.1 is used for all the calculation presented below. It should be noted here that for this cascade acoustic resonance was expected for s = 0° and 30° . However, for C10 airfoil geometry unsteady solutions were obtained with LNFLX2D for these interblade phase angles, unlike for the flat plate geometry mentioned in the previous section.

First, the amount of mistuning required to change the root locus plot is investigated i.e. whether the effects of 1% and 1.5% alternate as reported in Ref. 7 also occurs for this cascade. It should be noted here that the results from the present MISER code were checked with those given in Ref.7 for the 56 bladed cascade before starting the current calculations. Figure 6 shows the root locus plot with 1%,1.5%,5%,10% and 20% alternate mistuning for the flat plate geometry for M=0.7 and k_b = 0.18. It can be seen that an alternate mistuning of 1-10% did not show any effect on the eigenvalues. Only 20% alternate mistuning showed some effect on the eigenvalues. This is in contrast to the level of mistuning used in Ref. 7. However, Ref. 7 has considered a 56 bladed cascade in incompressible flow for which the cascading effect is much stronger.

However, the large amount of mistuning required here to have a significant effect on the eigenvalues (shown in Fig. 6) is not surprising. Similar values of mistuning have been used in Ref. 8. That study used an amount of 1 to 20% mistuning. An examination of Fig. 11 of Ref. 8 showed that the effect of alternate mistuning decreased with increasing Mach number. In light of study of Ref. 8 and the present results, it is concluded that for the Mach numbers considered here a mistuning of more than 20% has to be used to show a significant effect of mistuning. Therefore the rest of the calculations are done with 20% alternate mistuning.

Figure 7 shows the root locus plot obtained for the

C10 airfoil for both tuned and 20% alternate mistuning, for M=0.7 and k_b = 0.1. Comparison with flat plate geometry is also shown. The following are noted form Fig. 7: (1) For the tuned cascade both flat plate geometry cascade and C10 airfoil cascade are unstable for σ=60°. However, the C10 cascade is less unstable than the flat plate cascade. This indicates that for the tuned cascade the airfoil steady loading effects are stabilizing, compared to that for a flat plate airfoil; (2) the addition of 20% alternate mistuning moved the cascade with C10 geometry from an unstable to a stable condition, where as the flat plate cascade remained unstable; (3) It can also be seen that from the root locus plot for the C10 airfoil with mistuning, two frequencies are identified with σ=240° mode, whereas σ=60° mode is completely missing. The reason for this behavior is under investigation.

The root locus plot for M=0.8 and k_b = 0.1 is shown in Fig. 8. The following are noted form Fig. 8: (1)the tuned flat plate geometry cascade was unstable for σ=90° and C10 airfoil cascade was stable. This indicates that the airfoil steady loading effects are stabilizing for the tuned cascade, compared to that for a flat plate airfoil; (2) the addition of alternate mistuning made the C10 geometry more stable, where as the flat plate cascade remained unstable; (3) For the C10 airfoil it was noted that for tuned case both σ=90° and σ=120° modes have the same amount of damping, but with mistuning, σ=90° mode became more stable than the σ=120° mode.

CONCLUDING REMARKS

A two dimensional unsteady linearized aerodynamic Euler solver, LINFLX2D was used to calculate unsteady aerodynamic forces on oscillating cascades. The unsteady aerodynamic forces were used in the aeroelastic stability code MISER to calculate flutter characteristics. Results were presented for cascades in subsonic and transonic flow. The linearized Euler solver showed good correlation with the published data. The following were observed during the study.

(1) the airfoil steady loading stabilized the cascade for the Mach numbers considered.

(2) A relatively high amount of alternate mistuning is required to have an effect on the stability of the cascade for the Mach numbers considered.

(3 An accurate steady solution called "low loss solution " is required for the unsteady solver LINFLX2D to work. This requires a considerable amount of computational time. This may be the biggest drawback of using this code in a design cycle.

(4) The success of getting an unsteady solution from LINFLX2D also depended on the grids used.

(5) For predicting flutter boundary, calculations have to be done for a range of reduced frequencies. It is suggested that LINFLX2D data base be prepared for three or four reduced frequencies, and then use interpolation for flutter calculations. These reduced frequency values can be selected by first running MISER with linear theory.

(6) The unsteady solution times varied from 20 minutes to 75 minutes on an SGI workstation. This is directly related to the number of iterations required for convergence. A solution for flat plate geometry took more time than for the C10 airfoil geometry.

REFERENCES

(1)Reddy, et al, "A review of Recent Aeroelastic Analysis Methods for Propulsion at NASA Lewis Research Center", NASA TP 3406, December 1993.

(2)Whitehead, D.S., "Classical Two-Dimensional Methods", Chapter II in AGARD Manual on Aeroelasticity in Axial Flow in Turbomachines, Vol. 1, Unsteady Turbomachinery Aerodynamics, (ed. M. F. Platzer and F. O. Carta), AGARD-AG-298, pp. 3-1:3-30, Mar. 1987.

(3)Smith, S. N., "Discrete Frequency Sound Generation in Axial Flow Turbomachines," British Aeronautical Research Council, London, ARC R&M No. 3709, 1971.

(4)Adamczyk, J.J. and Goldstein, M.E., "Unsteady Flow in a Supersonic Cascade with Subsonic Leading-Edge Locus", ***AIAA Journal***, Vol. 16, No.12, pp. 1248-1254, Dec. 1978.

(5)Surampudi, S. P. and Adamczyk, J. J., "Unsteady Transonic Flow over Cascade Blades", ***AIAA Journal***, Vol. 24, No. 2, Feb. 1986, pp. 293-302.

(6)Lane, F., "Supersonic Flow past an Oscillating Cascade with Supersonic Leading-Edge Locus", ***Journal of the Aeronautical Sciences***, Vol. 24, pp .65-66, Jan. 1957.

(7)Kaza, K. R. V. and Kielb, R. E., "Flutter and Response of a Mistuned Cascade in Incompressible Flow," ***AIAA Journal***, Vol. 20, No. 8, pp. 1120-1127, 1982.

(8)Kielb, R. E. and Kaza, K. R. V., "Aeroelastic Characteristics of a Cascade of Mistuned Blades in Subsonic and Supersonic Flows", ***ASME Journal of Vibration, Acoustics, Stress and Reliability of Design***, Vol. 105, pp. 425-433, Oct. 1983.

(9)Verdon, J. M., "Linearized Unsteady Aerodynamic Theory," Chapter II in AGARD Manual on Aeroelasticity in Axial Flow in Turbomachines, Vol. 1, Unsteady Turbomachinery Aerodynamics, (ed. M. F. Platzer and F. O. Carta), AGARD-AG-298, pp. 2-1:2-31, Mar. 1987.

(10)Verdon, J.M. and Caspar, J.R., "Development of a Linear Unsteady Aerodynamic Analysis for Finite Deflection Subsonic Cascades", ***AIAA Journal***, Vol. 20, pp. 1259-1267, 1982.

(11)Hoyniak, D., Verdon, J.V., "Steady and Linearized Unsteady Transonic Analyses of Turbomachinery Blade Rows", Unsteady Aerodynamics and Aeroelasticity of Turbomachines, Y. Tanida and M. Namba (editors), pp. 109-124, 1995.

(12)Smith, T. E. and Kadambi, J. R., "The Effect of Steady Aerodynamic loading on the Flutter Stability of Turbomachinery Blading", ASME Paper 91-GT-130, 1991.

(13)Hall, K.C. and Clark, W.S., "Linearized Euler Predictions of Unsteady Aerodynamic Loads in Cascades", ***AIAA Journal***, vol. 31, No. 3, pp. 540-550, March 1993.

(14) Holmes, D.G. and Chuang, H.A., "2D Linearized Harmonic Euler Flow Analysis for Flutter and Forced Response", Unsteady Aerodynamic, Aeroacoustics, and Aeroelasticity of Turbomachines and Propellers, pages 213-230, Ed. Atassi, H.M, Springer-Verlag, New York, 1993

(15) Kahl, G. and Klose, "Computation of Time Linearized Transonic Flow in Oscillating Cascades", ASME Paper 93-GT-269, 38th IGT and Aeroengine Congress and Exposition, Cincinnati, Ohio, May 24-27, 1993.

(16) Verdon, J.V., Montgomery, M.D. and Kousen, K.A., "Development of a Linearized Unsteady Euler Analysis for Trubomachinery Blade Rows", NASA CR 4677, June 1995.

(17) Swafford, T.W., et al, "The Evolution of NPHASE: Euler/ Navier-Stokes Computations of Unsteady Two Dimensional Cascade Flow Fields", AIAA Paper 94-1834, 12th Applied Aerodynamics Conference, Colorado Springs, Colorado, June 20-23, 1994

(18) Lane, F., "System Mode Shapes in the Flutter of Compressor Blade Rows," ***Journal of the Aeronautical Sciences***, Vol. 23, pp. 54-66, Jan. 1956.

(19) Verdon, J.M., "The Unsteady Aerodynamic Response to Arbitrary Modes of Blade Motion", ***Journal of Fluids and Structures***, Vol. 3, pp. 255-274, 1989.

(20) Capece, V., personal communication, University of California, Davis, 1997

ACKNOWLEDGMENTS

This work is supported by a grant from Machine Dynamics Branch under funding form Advanced Subsonic Technology Project and Smart Green Engine Project. George Stefko, John Rohde and Kestutis Civinskas are the technical monitors.

Table 1

Unsteady Aerodynamic Force Coefficients

s/c=1.0, stagger=45°, σ=180°, k_b =0.5, x0=0.5
airfoil=10th standard configuration

			plunging	pitching
flat plate M=0.7	cl	a	-3.56752,1.29455	-4.244,.73506
		b	-3.5133,1.2338	-4.1786,.6609
	cm	a	0.55951,-.67647	.71385,-.87771
		b	0.5297,-0.6417	.6780,-.8324
airfoil M=0.7	cl	a	-3.5675,1.29455	-4.2439,.73506
		b	-2.5502,-0.0132	-2.2566,-.1537
		c	-2.6370,0.0553	-2.3040,-.0487
		d	-2.6576,0.0310	-2.4415,-.0362
	cm	a	0.5595,-.67647	0.71385,-.87771
		b	.6497,-.3330	0.6001,-0.4540
		c	.6124,-.3340	0.5513,-0.4406
		d	.6346,-.3474	0.5917,-0.5108
airfoil M=0.8	cl	a	-.47916,2.64057	-.4467,3.10392
		b	*	*
		c	-2.5945,1.0469	-1.8953,0.8885
		d	-2.7240,1.1272	-2.0532,0.9119
	cm	a	-.46335,0.03245	-.78786,-.16579
		b	*	*
		c	0.3352,-0.6922	0.2215,-0.6712
		d	0.3615,-0.6567	0.2657,-0.6940

a=linear theory, Ref. 3, b=LINFLX2D (155x41 grid),c=LINFLX2D (141x41 grid)
d=nonlinear unsteady Euler code, Ref. 17

* could not get solution with this grid

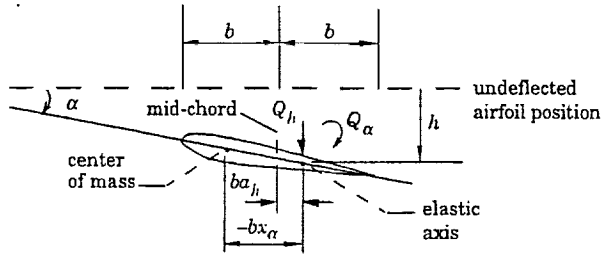

Figure 1: Typical section blade model with two degrees-of-freedom.

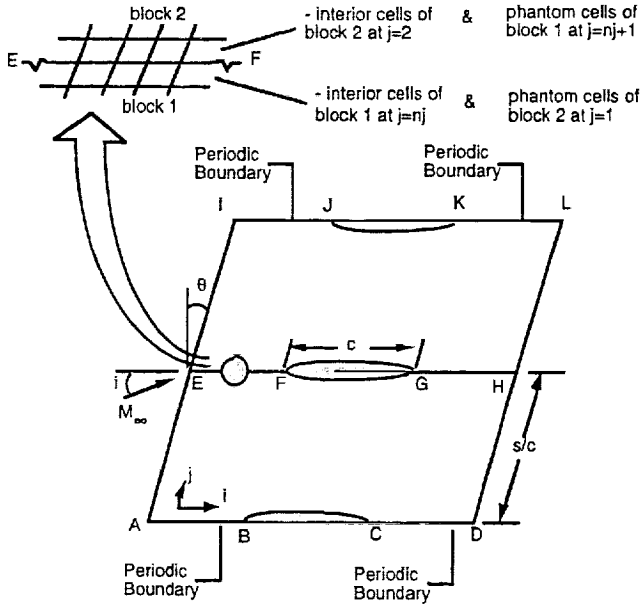

Figure 2: Cascade geometry showing stagger angle (θ), chord length (c), incidence angle (i) and spacing (s), periodic and injection boundaries used in calculations with multiple grid blocks.

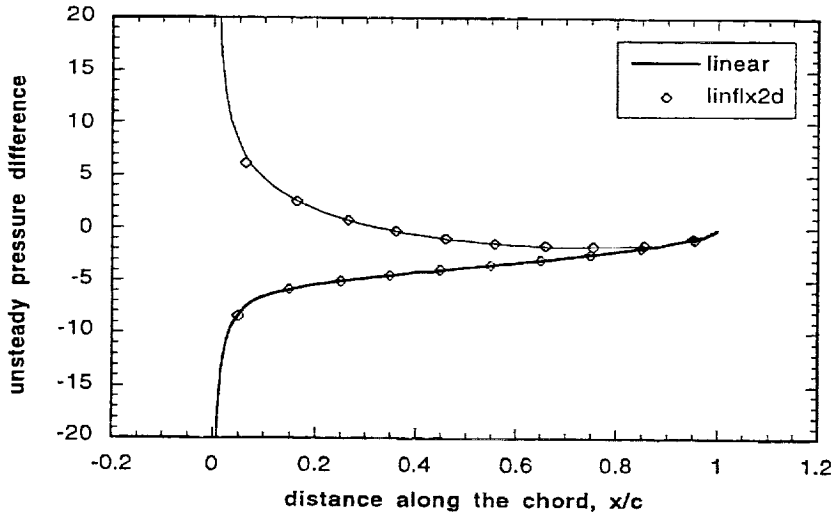

Figure 3a: Unsteady pressure difference distribution for a flat plate geometry cascade; pitching about mid-chord; , $s/c = 1.0$, $\theta = 45°$, $M_\infty = 0.7$, $i = 0°$, $k_b = 0.5$, $\sigma = 180°$

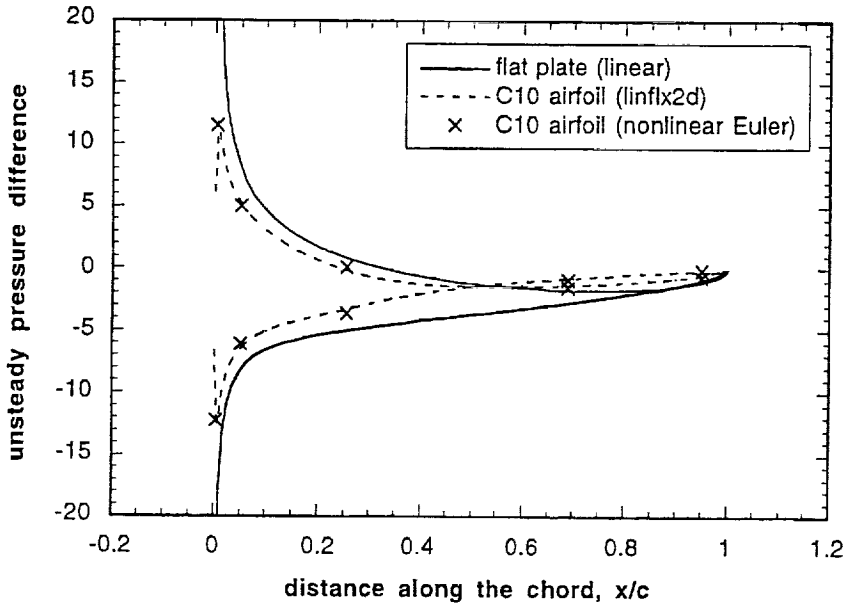

Figure 3b:Unsteady pressure difference distribution for a subsonic cascade, pitching about midchord; , $s/c = 1.0$, $\theta = 45°$, $M_\infty = 0.7$, $i = 10°$.$k_b = 0.5$, $\sigma = 180°$, $\alpha_o = 2°$

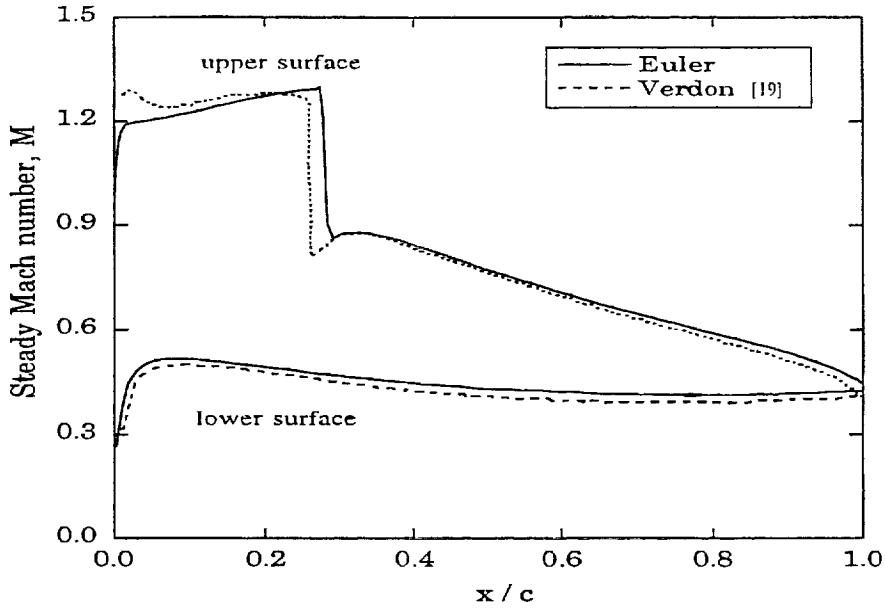

Figure 4a: Steady Mach number distribution for a transonic cascade; standard configuration No. 10, $s/c = 1.0$, $\theta = 45°$, $M_\infty = 0.8$, $i = 13°$.

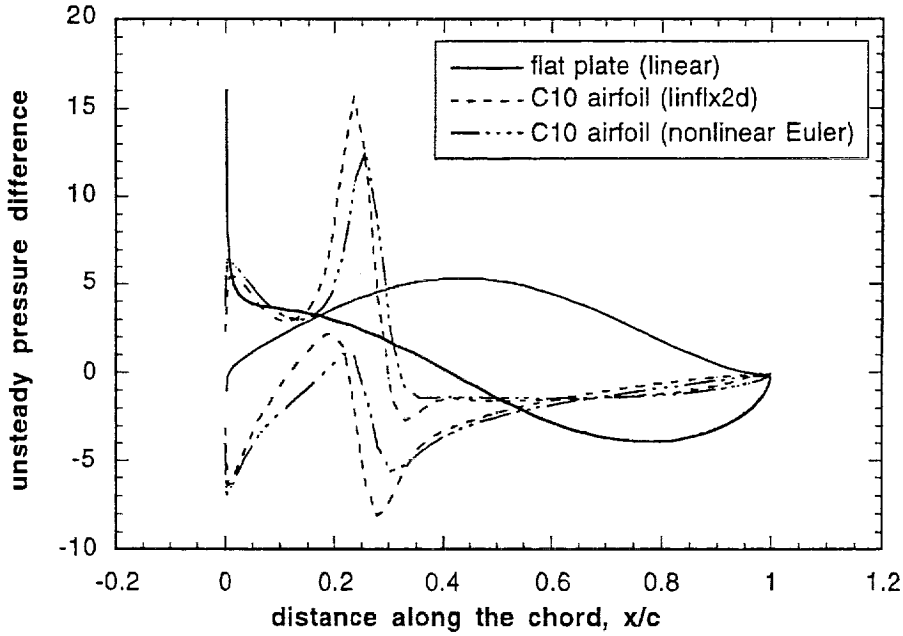

Figure 4b: Unsteady pressure difference distribution for a transonic cascade; standard configuration No. 10, pitching about mid-chord; parameters as in Fig. 4a, $k_b = 0.5$, $\sigma = 180°$, $\alpha_0 = 2°$.

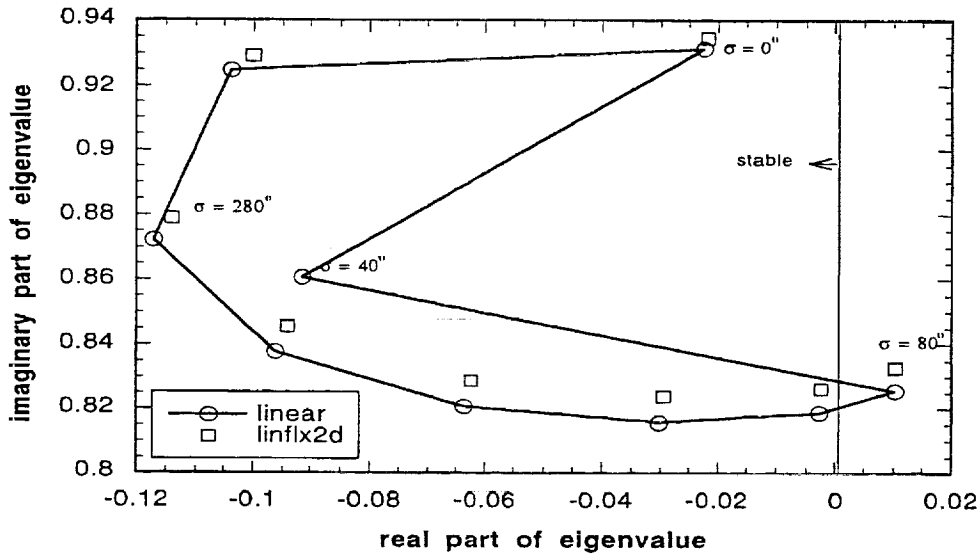

Figure 5: Root locus plot for 9 bladed cascade, torsional motion, flat plate geometry, $k_b = 0.18$, a=0.0, μ=258.5, $r_a = 0.5774$, structural damping=0.0, M=0.7, $i = 10°$, $\omega_h/\omega_\alpha = 0.357$

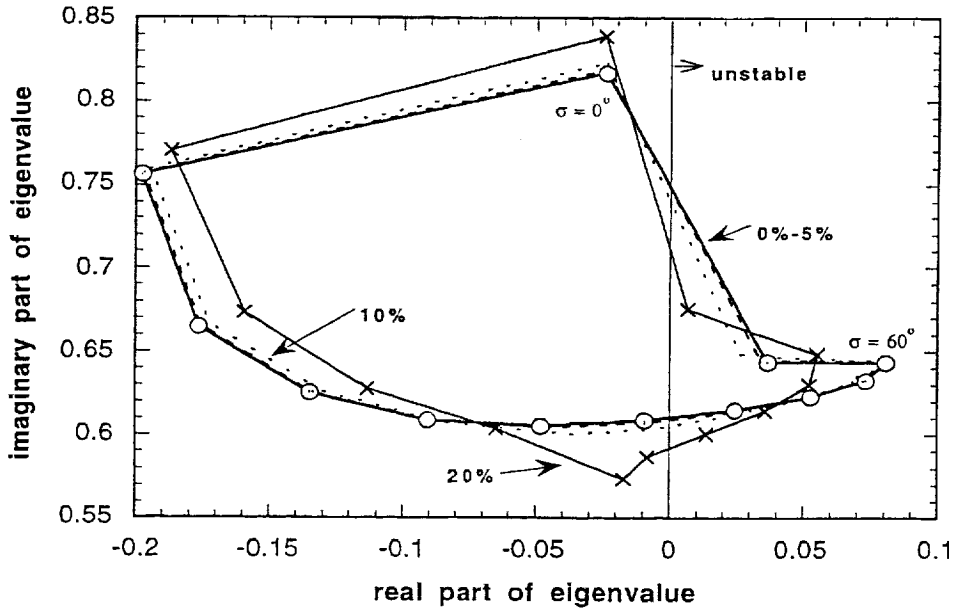

Figure 6: Effect of alternate mistuning on eigenvalues in subsonic flow; flat plate geometry, $M_\infty = 0.7$, $i = 10°$, $k_b = 0.1$,.N=12, pitching about mid-chord; .1%,2%,5%,10%, 20%; structural parameters same as in Fig.5

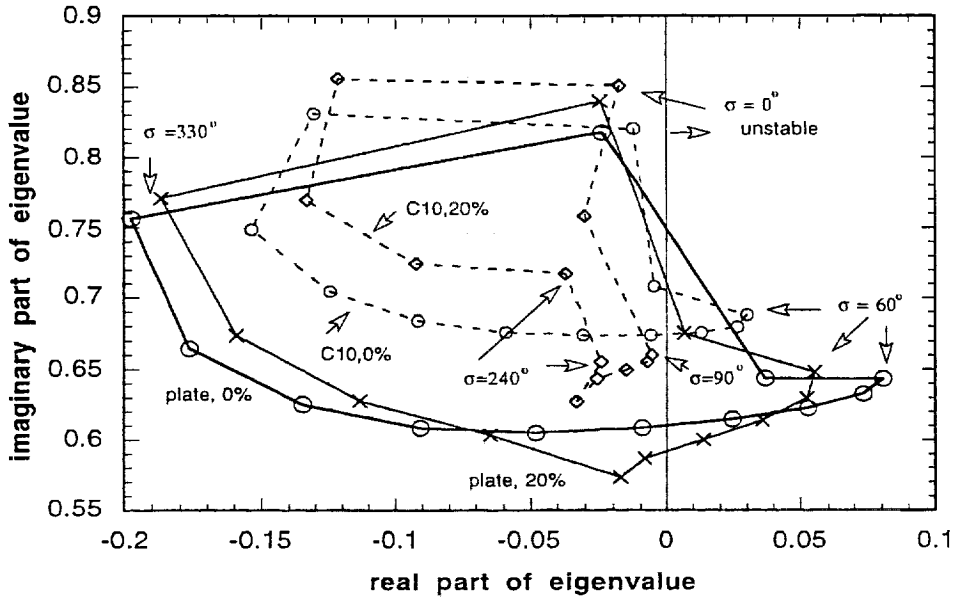

Figure 7: Effect of alternate mistuning on eigenvalues in subsonic flow; standard configuration No. 10, $M_\infty = 0.7$, $i = 10°$, $k_b = 0.5$,.N=12, pitching about mid-chord; structural parameters same as in Fig.5

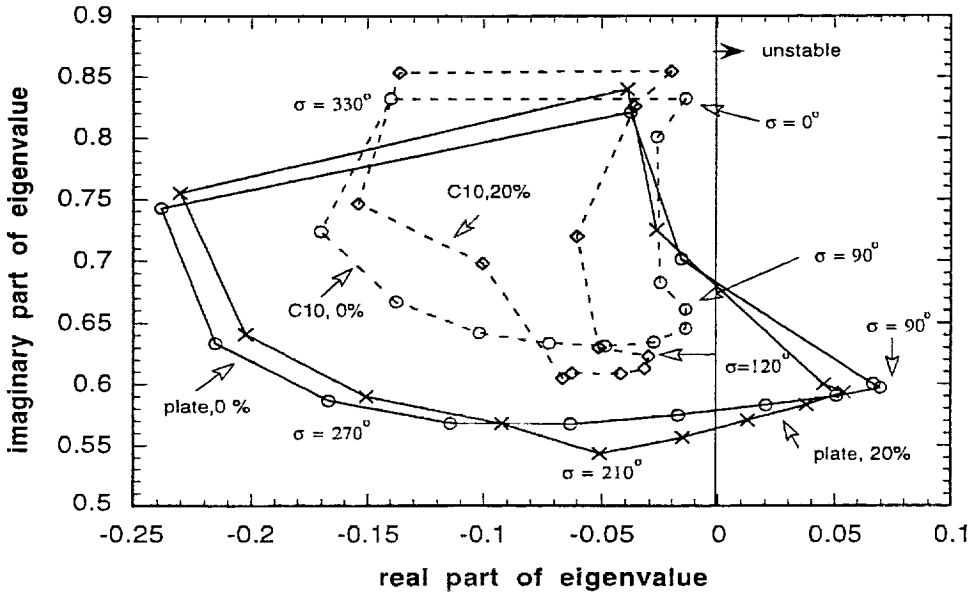

Figure 8: Effect of alternate mistuning on eigenvalues in transonic flow; standard configuration No. 10, $M_\infty = 0.8$, $i = 13°$, $k_b = 0.1$,.N = 12, pitching about mid-chord; structural parameters same as in Fig. 5

AIAA-99-2679

ASTROP2-LE: A Flutter and Forced Response Analysis System Based on a 2D Linearized Euler Solver

T. S. R. Reddy
R. Srivastava

The University of Toledo
Toledo, Ohio

O. Mehmed

NASA Glenn Research Center
Cleveland, Ohio

35th AIAA/ASME/SAE/ASEE Joint Propulsion Conference and Exhibit
20–24 June 1999
Los Angeles, California

AIAA-99-2679

ASTROP2-LE: A FLUTTER AND FORCED RESPONSE ANALYSIS SYSTEM BASED ON A 2D LINEARIZED EULER SOLVER

T.S.R. Reddy*, R. Srivastava*
The University of Toledo
Toledo, OH

O. Mehmed+
NASA Glenn Research Center
Cleveland, OH

Abstract

A flutter and forced response analysis system based on a two-dimensional linearized Euler solver was developed. The ASTROP2 code, an aeroelastic stability analysis program for turbomachinery, was used for this purpose. The ASTROP2 code uses strip theory to couple a two dimensional aerodynamic model with a three dimensional structural model. The code was first modified to include forced response capability. The unsteady aerodynamic modeling of the ASTROP2 was also changed to accept the loads from a linearized Euler solver, LINFLX2D. By including the unsteady aerodynamic loads from LINFLX2D, it is possible to include the effects of transonic flow on flutter and forced response in the analysis. The updated code, ASTROP2-LE for ASTROP2 code using Linearized Euler aerodynamics, is validated by comparing the predictions with those obtained using linear unsteady aerodynamic solutions.

Introduction

The aeroelastic research program at NASA Glenn Research Center is focused on flutter, and forced response analysis of turbomachinery. An overview of this research was presented in Ref. 1. The review showed that a range of aerodynamic and structural models have been used to obtain the aeroelastic equations. Both time and frequency domain methods have been used to obtain unsteady aerodynamic forces and to solve the aeroelastic equations. It was noted that time domain methods require large computational time compared to frequency domain methods, and should only be used when non-linearities are expected, and when the need justifies the cost.

* Senior Research Associate, Member AIAA
+ Research Engineer, Member AIAA

Two approaches were used in obtaining the unsteady aerodynamic forces using frequency domain methods. In the first approach, Ref. 2, the unsteady aerodynamic equations are linearized about a uniform steady flow, there by neglecting the effects of airfoil shape, angle of attack and thickness. The unsteady aerodynamic models developed in Refs. 3-6 based on this approach are used in Refs. 7-8 to study the flutter and forced response analysis of a compressor rotor using a typical section structural model. Some of these models were also integrated with a three dimensional structural model using strip theory in Ref. 9. However, methods developed by this approach are restricted to shock-free flows and lightly loaded blade rows.

In the second approach, Ref. 10, the unsteady flow is regarded as a small amplitude perturbation about a non-uniform steady flow. The unsteady non-linear aerodynamic equations are linearized about the non-uniform steady flow, resulting in variable coefficient linear unsteady aerodynamic equations, which include the effects of steady aerodynamic loading due to airfoil shape, thickness and angle of attack. Following the second approach, Refs. 11-13 developed a steady and linear unsteady aerodynamic model based on the potential equation. This unsteady aerodynamic model was used to study the effect of steady aerodynamic loading on flutter stability using a typical section structural model in Ref. 14. Subsequently this aerodynamic model was integrated with a three dimensional structural model using strip theory in Ref. 15.

However, the formulation based on the potential equation requires corrections for entropy and flow rotation. The Euler equations can be used to correctly model rotational and entropy effects associated with strong shocks. Unsteady linearized Euler aerodynamic models that include the effect of steady aerodynamic loading were developed in Refs. 16-18. Recently, a two-dimensional linearized Euler code, LINFLX2D, was developed under a NASA contract and has been reported in reference 19. This code is based on the non-linear Euler solver developed in Ref. 20. In Ref.

21, the unsteady aerodynamic calculations from LINFLX2D were coupled with MISER (Ref. 7); a frequency domain aeroelastic stability and response code based on a typical section structural model. Flutter and forced response calculations were presented for cascades in subsonic and transonic flow, with and without mistuning.

The aeroelastic formulation in MISER does not represent the behavior of a three dimensional structure. An ideal analysis will be to couple a three dimensional structural analysis with a three dimensional aerodynamic analysis. This may be computationally intensive. An intermediate approach that couples a two dimensional aerodynamic analysis with a three dimensional structural model using strip theory, quasi-3D approach, may be less expensive computationally. This approach will provide accurate results except where three dimensional effects dominate. In turbomachines, where the compressors and turbines are enclosed, three-dimensional effects may not be strong, and strip theory can be used. The ASTROP2 code reported in Ref. 9 uses this strip analysis approach for aeroelastic stability analysis.

The primary objective of the present study is to develop a quasi-3D aeroelastic code by coupling the LINFLX2D code with a three dimensional structural model using strip theory. This effort uses the ASTROP2 code of Ref. 9 as the basis. The ASTROP2 code is a frequency domain stability analysis program, and as mentioned before uses strip theory to couple a two dimensional aerodynamic model with a three dimensional structural model. The present version of ASTROP2 has provision for flutter calculations, but not forced response. During the course of the research effort, the ASTROP2 code is extended to include forced response calculation. The resulting code is named ASTROP2-LE for ASTROP2 code using Linearized Euler aerodynamics. Brief descriptions of the formulation and method of analysis are given in the next section, followed by results and discussion.

Formulation

The aeroelastic formulation using the linearized approach requires solutions from two aerodynamic codes and a solution from a structural dynamic analysis code. The steady aerodynamic loads are obtained from a non-linear Euler solver, NPHASE, and the unsteady loads are obtained from LINFLX2D. The structural dynamic solution can be obtained from any finite element code, analytical solutions or measured data. The salient features of both the aerodynamic codes, and the aeroelastic formulation are described below.

Aerodynamic model

Non-linear Steady Euler Solver, NPHASE

The steady aerodynamic model is based on the unsteady, two dimensional, non-linear Euler equations. The equations in conservative differential form are solved in a time dependent body-fitted curvilinear reference frame. This transformation process and the ensuing numerical method are presented in detail in Ref. 20. The equations are discretized and solved using a finite volume method using a combination of flux difference splitting and flux vector splitting scheme. In addition, limiters are used to control dispersive errors commonly encountered with higher order schemes. The steady solutions presented herein are obtained using the basic implicit scheme developed in Ref. 20, which is third order accurate spatially and second order accurate in time.

Linear Unsteady Euler Solver, LINFLX2D

To obtain the linearized unsteady Euler equations, the independent variables in the unsteady non-linear Euler equations are expanded in an asymptotic series of the form

$$U = U(x) + u(x(x,t),t) + \text{ higher order terms} \qquad (1)$$

Assuming the unsteady excitations are harmonic in time, and with the first order variable to be represented as complex valued, the above equation can be written as

$$U = U(x) + \mathrm{Re}[u(x)\exp(i\omega t)] + \text{higher order terms} \qquad (2)$$

Here, the term U(x) is of order one and the second term is of the order ε.

Substituting the expansion of Eq. 2 in the non-linear unsteady Euler equations, and equating terms of like power in ε, and neglecting terms of second and higher order in ε, nonlinear steady equations and linear variable coefficient unsteady equations are obtained.

For harmonic blade motions with constant phase angle between adjacent blades (interblade phase angle), the values of interblade phase angle (σ) that can occur are given in Ref. 22 as

$$\sigma_r = 2\pi r / N \qquad r=0,1,2,\ldots,N-1 \qquad (3)$$

where N is the number of blades in the cascade. In a time domain approach, the number of blocks required depends on the interblade phase angle, and small phase angles may require large number of blocks to

calculate the unsteady aerodynamic forces. However, with the linearized approach, the periodic conditions are applied on a single extended blade passage region i.e., a region of angular pitch,

$$\theta = 2\pi / N \tag{4}$$

In solving the linear unsteady equations, the independent variables are regarded as pseudo time dependent. This allows solutions to be determined using conventional time marching algorithms to converge the steady and the complex amplitudes of the unsteady conservation variables to their steady state values. For more details, see reference 19.

Aeroelastic Model

As mentioned before, the primary objective of the present study is to couple the LINFLX2D solver with a three dimensional structural model using strip theory. For this effort, the ASTROP2 code of Ref. 9 is selected as the basis.

The ASTROP2 code uses strip theory to couple a two dimensional aerodynamic model with a three dimensional structural model. The present version of ASTROP2 can solve only for flutter and not for forced response. For clarity and completeness, the aeroelastic formulation in ASTROP2 is given here with extension to include forced response calculation.

ASTROP2 uses the normal mode approach for aeroelastic analysis. The equations of motion for the s^{th} blade of the cascade, Fig. 1a, can be written as

$$[M_{gs}]\{\ddot{q}_s\} + [K_{gs}]\{q_s\} = [A_s]\{q_s\} + \{AD_s\} \tag{5}$$

where $[M_{gs}]$ and $[K_{gs}]$ are generalized mass and stiffness matrices, which are diagonal, $\{q_s\}$ is the generalized displacement vector, and $[A_s]$ is the motion dependent generalized aerodynamic load matrix, and $\{AD_s\}$ is the motion independent generalized aerodynamic load vector. The motion dependent forces cause flutter, and motion independent forces cause forced response (forced vibration). The matrices $[M_{gs}]$, $[K_{gs}]$, and $[A_s]$ are of NM x NM size, $\{q_s\}$ and $\{AD_s\}$ are of NM x 1 size, where NM is the number of normal modes used in the analysis. The matrices $[M_{gs}]$ and $[K_{gs}]$ are given by a free vibration analysis. It should be noted that in the stiffness matrix, the structural damping could be added by multiplying the stiffness coefficients by $(1+2i\varsigma_s)$, where ς is structural damping ratio. The expressions for $[A_s]$ and $\{AD_s\}$ are given below.

In ASTROP2 the blades are divided into strips where the aerodynamic forces are calculated. Each strip has two degrees of freedom, a plunging displacement, h, motion perpendicular to chord, and a pitching (torsion) displacement, α, rotation about the leading edge of the strip (Fig. 1b).

Using the normal modal values obtained from a free vibration analysis, the equivalent h and α for k^{th} strip of the s^{th} blade are given as summation of normal modes as

$$\{u_{sk}\} = \begin{Bmatrix} h \\ \alpha \end{Bmatrix} = \begin{bmatrix} h_1 h_2 .... h_{NM} \\ \alpha_1 \alpha_2 .... \alpha_{NM} \end{bmatrix} \{q_s\} = [W_k]\{q_s\} \tag{6}$$

As mentioned before, an N blade cascade can vibrate in N interblade phase angles given by Eq. 3. The aerodynamic forces at each strip for the r^{th} interblade phase angle mode can be written as a sum of motion dependent and motion independent forces as

$$[L_{rk}] = [L1_{rk}] + \{L2_{rk}\} \tag{7.1}$$

where

$$[L1_{rk}] = \begin{bmatrix} l_{hhr} & l_{h\alpha r} \\ l_{\alpha hr} & l_{\alpha\alpha r} \end{bmatrix} \{u_{sk}\} = \begin{bmatrix} l_{hhr} & l_{h\alpha r} \\ l_{\alpha hr} & l_{\alpha\alpha r} \end{bmatrix} [W_k]\{q_s\}$$

$$\{L2_{rk}\} = \begin{Bmatrix} l_{whr} \\ l_{w\alpha r} \end{Bmatrix} \tag{7.2}$$

where the subscript 'w' refers to force from wake i.e. motion independent aerodynamic forces. The values of l_{hhr}, $l_{h\alpha r}$, $l_{\alpha hr}$, $l_{\alpha\alpha r}$, l_{whr}, and $l_{w\alpha r}$ for a given interblade phase angle are calculated from the unsteady aerodynamic forces obtained from linear theory, Ref. 4 or LINFLX2D, Ref. 19.

The generalized aerodynamic matrices $[A_{sr}]$ and $\{AD_{sr}\}$ for the entire blade are given by

$$[A_{sr}] = \int [W_k]^T [L1_{rk}] ds = \int_0^L [A_{srk}] ds_k \tag{8.1}$$

$$\{AD_{sr}\} = \int [W_k]^T \{L2_{rk}\} ds = \int_0^L [AD_{srk}] ds \tag{8.2}$$

where L is the blade length and T indicates transpose.

Integrals in Eq. 8 are evaluated using numerical integration as

$$[A_{sr}] = \sum_{k=1}^{NSTRIP} [A_{srk}] ds_k \tag{9.1}$$

$$\{AD_{sr}\} = \sum_{k=1}^{NSTRIP} \{AD_{srk}\} ds_k \tag{9.2}$$

where ds_k is the strip width, and NSTRIP is the number of strips the blade is divided into.

For a tuned cascade, in which all the blades are identical structural properties, the interblade phase angle modes are uncoupled. In this case, the aeroelastic modes consist of individual blades vibrating with equal amplitudes with a fixed interblade phase angle between adjacent blades. Hence, for this problem, the motion of the typical blade is written as

$$\{q_s\} = \{q_{0s}\} e^{i\omega t} = \{q_{ar}\} e^{i\omega t} e^{i\sigma_r s} \tag{10}$$

The equations of motion for the blade for each interblade phase angle can be written as

$$\begin{aligned} &-\omega^2 [M_{gs}] \{q_{ar}\} e^{i(\omega t+\sigma_r s)} + [K_{gs}] \{q_{ar}\} e^{i(\omega t+\sigma_r s)} \\ &= \omega^2 [A_r] \{q_{ar}\} e^{i(\omega t+\sigma_r s)} + \omega^2 [AD_r] e^{i(\omega t+\sigma_r s)} \end{aligned} \tag{11}$$

The matrices $[M_{gs}]$, $[K_{gs}]$, and $[A_r]$ are of NM x NM size, $\{q_{ar}\}$and $\{AD_r\}$ are of NM x 1 size. Since the blades are identical, the same equation is obtained for each blade; equation 11 can be solved for N different values of the interblade phase angle given by Eq. 3.

Dividing both sides by an assumed frequency, ω_0^2, dropping the subscripts, and rearranging, the equations can be written as

$$[[P] - \gamma[Q]]\{q_{ar}\} = \gamma\{AD\} \tag{13}$$

where

$$\begin{aligned} [P] &= \frac{1}{\omega_0^2}[K] \\ [Q] &= [[M] + [A]] \end{aligned} \tag{14}$$

and

$$\gamma = \left(\frac{\omega}{\omega_0}\right)^2$$

For a stability calculation (flutter), the motion-independent forces {AD} are set to zero and the eigenvalue problem is obtained as

$$[[P] - \gamma[Q]]\{q_{ar}\} = \{0\} \tag{15}$$

The solution of the above eigenvalue problem results in NM complex eigenvalues of the form

$$i\left(\frac{\omega}{\omega_0}\right) = i\sqrt{\gamma} = \mu + i\nu \tag{16}$$

The real part of the eigenvalue (μ) represents the damping ratio, and the imaginary part (ν) represents the damped frequency; flutter occurs if $\mu \geq 0$ for any of the eigenvalues. The eigenvalue problem is solved for each of the N permissible values. The critical phase angle is identified as the one that results in the lowest flutter speed.

The aeroelastic response of the blades induced by wakes is calculated from equation (13) as

$$\{q_{ar}\} = -[[P] - \gamma[Q]]^{-1} \gamma\{AD\} \tag{17}$$

Stability calculation procedure

The aerodynamic coefficients are calculated before the eigenvalue problem can be set up and solved. Since the unsteady aerodynamic coefficients depend on the frequency of oscillation, it is necessary to assume a frequency ω_0 (actual input to the code may be the reduced frequency of blade vibration based on chord, $k_c = \omega c / U$, where U is the free stream velocity) in advance to be able to calculate the aerodynamic coefficients. The aerodynamic coefficients are functions of inlet Mach number M, and interblade phase angle σ_r, in addition to cascade geometric parameters. In the present study, for a given inlet Mach number, the reduced frequency is varied until the real part of one of the eigenvalues μ becomes zero while the real parts of the remaining eigenvalues are negative. The assumed flutter-reduced frequency k_{cf} and the calculated flutter frequency ν_f are both based on ω_f. Thus, these two can be combined to eliminate ω_f and the flutter speed is obtained, namely, $\nu_f c\omega_0 / k_{cf}$. Since the inlet Mach number is known, this flutter speed gives the inlet condition (speed of sound, a_∞) at which the cascade will be

neutrally stable for the given Mach number. This procedure can be repeated to obtain a plot of flutter speed versus Mach number. Knowing the operating conditions, it is possible to determine whether flutter will occur within the operating region and if so, the Mach number and frequency at flutter.

Analysis procedure

The flutter and forced response analysis in ASTROP2-LE consists of running five codes, (I) a structural dynamic analysis code, (II) 2DSTRIP, (III) NPHASE, (IV) LINFLX2D, and (V) 2DASTROP. It is to be noted that ASTROP2 code is a combination of 2DSTRIP and 2DASTROP codes. The analysis procedure is explained in five steps. In step 1 a vibration analysis is performed for the blade. The output is natural frequencies and mode shapes. This output is used by 2DSTRIP. In step 2, strips are selected, and 2DSTRIP is run to calculate relative Mach numbers, sweep angles, stagger angles, chord values, and strip widths at these strips. During this run, the three dimensional modal values are also interpolated at each strip, and equivalent pitching and plunging modal values are calculated. In step 3, a steady aerodynamic solution at these strips is obtained from NPHASE. The steady aerodynamic solution is written as a database. Step 4 consists of running LINFLX2D for assumed number of reduced frequencies, interblade phase angles, for pitching and plunging modes. The analysis is carried out for unit amplitude of vibration for all the strips, and the unsteady aerodynamic solutions are stored as a database. In step 5, the 2DASTROP code is executed to calculate flutter using the eigenvalue approach and to calculate forced response.

Strategy to reduce the number of calculations

The main purpose of the present effort is to accurately couple the unsteady aerodynamic solutions from LINFLX2D to ASTROP2 code. In order to reduce the number of calculations, the following observations are made on the number of calculation required for flutter.

Let each blade be divided into NSTRIP number of strips. In general, for a given inlet Mach number, the flow conditions, (relative Mach number and angle of attack), and the geometric conditions, (gap to chord ratio, stagger angle, and airfoil shape) are different at these strips. Therefore, the number of steady aerodynamic solutions (number of NPHASE runs) required is (NSTDY = NSTRIP * NMACH), where NMACH is the number of inlet Mach numbers to be considered in the study. By considering a straight, untapered stator blade, the flow and geometric conditions will be same at all strips, reducing the number of steady aerodynamic calculations to NMACH, i.e. NSTDY=NMACH.

In the present study two inlet Mach numbers will be considered i.e. NMACH=2. Therefore the number of study runs is NSTDY = 2*NSTRIPS. Assuming identical flow and geometric conditions, the number of NPHASE (study solution) runs reduces to NSTDY = 2.

In the case of the unsteady aerodynamic solution, two other parameters, reduced frequency (k_c) and interblade phase angle (σ) have to be considered. If NREDF is the number of reduced frequencies, and NSIGMA is the number of interblade phase angles, then the number of unsteady solutions for flutter (number of LINFLX2D runs) is, NUSTDY = NMACH *NSTRIP *NSIGMA *NREDF. However, if same geometric and flow conditions are assumed at all strips, NUSTDY is reduced to NUSTDY = NMACH*NSIGMA*NREDF. It is to be noted here that NSIGMA is equal to the number of blades of the cascade.

For NMACH=2, the number of unsteady runs, NUSTDY= 2*NSTRIP*NREDF*NSIGMA. Again assuming identical flow and geometric conditions, NUSTDY=2*NREDF*NSIGMA.

Results and Discussion

Results presented here are meant to show that the analysis procedure given in the previous sections has been implemented correctly in LINFLX2D and ASTROP2. Therefore, calculations are made for a non-rotating cantilevered blade, representing a stator blade of a turbomachinery component. Results are presented for an assembly of 12 tuned blades on a rigid disk coupled only aerodynamically. Similar geometry was considered in Ref. 23. Two inlet Mach numbers are considered M=0.7 and 0.8. Two airfoils, a flat plate and the tenth standard configuration, C10 airfoil cross sections, Ref. 25, are considered. The gap to chord ratio (s/c) is 1.0 and the stagger angle is 45 degrees. For the C10 airfoil and for M=0.8, the flow is transonic with a shock near the quarter chord.

Code Validation:

ASTROP2 code:

The ASTROP2 code was validated for flutter prediction in Ref. 9 by calculating the flutter boundary of the SR3CX2 advanced propeller. The vibration characteristics of the propeller blade were obtained from the finite element structural analysis code NASATRAN. Linear theory of Ref. 5 was used for calculating the unsteady aerodynamic forces. The

predicted flutter Mach number was conservative compared to the measured value. For more details on the ASTROP2 code, see references 9, 24 and 25.

LINFLX2D code:

To validate the LINFLX2D code, unsteady aerodynamic pressure differences were calculated for a flat plate cascade, and a cascade comprising of C10 airfoils with inflow Mach numbers of M=0.7 and M=0.8, for a reduced frequency of oscillation based on chord (k_c) of 1.0. The unsteady pressure difference is non-dimensionalized by (upper surface pressure-lower surface pressure) / (airdensity*U**2*amplitude of oscillation). An H-grid of 141x41 grid is used for the study. There are 80 points on the airfoil, and the inlet boundary is 5 chords from the airfoil leading edge and the exit boundary is 10 chords from the airfoil trailing edge. Steady aerodynamic solutions were obtained for these Mach numbers using NPHASE before running LINFLX2D.

Subsonic Inflow

Figure 2a shows the steady Mach number distribution obtained for the C10 airfoil cascade for an inlet Mach number, M=0.7. The flow to the cascade is at 10 degrees angle of attack. It can be seen that for this Mach number the flow is shock free. The unsteady pressure difference distribution for an interblade phase angle, σ, of 180 degrees is shown in Fig. 2b. The blades are oscillating in pitch about the midchord. Figure 2b shows predictions from linear theory (Ref. 4) for flat plate geometry, from the nonlinear Euler (Ref. 20) and the linearized Euler code, LINFLX2D for the C10 airfoil geometry. The predictions from LINFLX2D correlate well with the nonlinear Euler results. As expected, the results show significant difference with linear theory, because the effects of airfoil geometry, and angle of attack are not included in the linear theory.

Figure 2b also shows the unsteady pressure difference distribution obtained with LINFLX2D for the flat plate geometry, and its correlation with linear theory. It can be seen that for the flat plate geometry results from linear theory and LINFLX2D match very well. At M=0.7 the flow field is linear; hence, linear theory and the linearized Euler results are expected to correlate well. This validates the LINFLX2D code for subsonic flows.

Transonic Inflow

For the C10 airfoil cascade geometry, and for an inlet Mach number of 0.8, the flow is transonic with a normal shock occurring in each blade passage. The steady Mach number distribution obtained from NPHASE is shown in Fig. 3a for a steady angle of attack of 13 degrees. A normal shock occurs on the suction surface at about 28% of the chord. Results from the full potential solver, Ref. 12, are also included for comparison. Both results agree well, except that the nonlinear steady Euler solver, NPHASE, predicts the shock location slightly downstream of that predicted by the full potential solver of Ref. 12. A shock fitting procedure was used in Ref. 12, whereas the shock is captured naturally in NPHASE.

The unsteady pressure distribution is shown in Fig. 3b, along with a comparison with linear theory (Ref. 4) and the unsteady nonlinear Euler solver. The unsteady results are for pitching about mid-chord with $k_c = 1.0$, $\sigma = 180°$ and amplitude of oscillation, α_0, = 2°. As expected, linear theory does not show any shock, indicating that unsteady analysis based on linear theory will not be accurate for cascade flutter analysis in transonic flow. Some discrepancy is seen between the unsteady results obtained from LINFLX2D and from the unsteady nonlinear Euler solver. For the transonic flow case the following factors may have more effect than for in subsonic case: (1) grids used, (2) accuracy lost when time series data is processed to obtain frequency data or (3) the steady solution on which LINFLX2D based is not a low loss solution. Even though these issues need separate study, Fig. 3b shows a fair correlation between LIFLX2D results and non-linear unsteady Euler.

Similar results were obtained for plunging motion for both subsonic and transonic inflows.

Stability and Response Calculations

As mentioned before, a 12 blade stator is considered for stability and response calculations. Since the main aim of this paper is to demonstrate the ASTROP2 and LINFLX2D code coupling, analysis is carried out for an assumed geometry of straight, untwisted stator blades at two inlet Mach numbers, 0.7 and 0.8. This reduces the number of steady runs, NSTDY, 2 (one for M=0.7 and one for M=0.8) and the number of unsteady runs, NUSTDY, to 24*NREDF for a 12 blade cascade. The same grids that were used for the unsteady validation and the NPHASE steady solution obtained in the previous section were used again.

The blade is divided into 10 strips (NSTRIP=10). Table 1 shows the aerodynamic input parameters, and table 2 shows the modal values used in this study. These are same as those used in Ref. 23. The modal values at the strips are used for generalized force calculation. Two modes are used in the analysis.

The first mode is a pure torsion mode and the second mode is a coupled bending-torsion mode. The natural vibration frequencies are 81.376HZ and 148.02 HZ respectively.

Stability calculation

The unsteady aerodynamic force coefficients are calculated using LINFLX2D for harmonic blade vibration in plunging and pitching modes for a reduced frequency, k_c, of 0.2 based on chord. The calculated unsteady force coefficients are used by 2DASTROP code to calculate the elements of [A]. With identical flow and geometric conditions, the only contribution to the generalized aerodynamic force matrix is due to the different modal values at different strips. The reduced frequency used to calculate the unsteady aerodynamic force coefficients, k_c=0.2, corresponds to a frequency of 96.07 HZ.

Figure 4 compares the root locus plot of the eigenvalues obtained from LINFLX2D with that obtained using linear theory unsteady aerodynamics for a flat plate geometry. The plot is shown for the first mode for M=0.7. Good correlation is observed. At M=0.7 the flow field is linear hence, linear theory and linearized Euler are expected to correlate well with each other. The linear theory unsteady aerodynamic code was an integral part of ASTROP2, and LINFLX2D is the new code that is coupled with ASTROP2. The root locus plot correlation shows that the coupling of the LINFLX2D unsteady aerodynamic database to ASTROP2 is accurate. It is to be noted that since the first mode is a pure torsional mode, the frequency of the aeroelastic system is close to the first natural frequency of the blade.

To explore the effects of airfoil shape and transonic flow the analysis was carried out with the C10 geometry and for M=0.7 and 0.8. Figure 5 shows the root locus plot for the first mode at an inflow M of 0.7 for the flat plate and C10 airfoil geometries. It can be seen that the blade is more unstable when the effect of airfoil geometry is included.

The root locus plot for the first mode for M=0.8 is shown in Fig. 6. Here the root locus plot shows the effect of both airfoil shape and transonic flow effects. It is seen that the blade is slightly more unstable than in figure 5 when the effects of airfoil geometry, and shock are included.

Response Calculations

The response of the blade to a vortical disturbance is calculated for flat plate geometry and C10 geometry and compared with that obtained from linear theory.

In general the response calculation can be done by including the motion dependent aerodynamic matrix, [A], which adds the contribution of aerodynamic damping to the response. The forced response is usually calculated for an aeroelastically stable system (positive aerodynamic damping), and the contribution of [A] to response can be ignored. For the calculations presented here, the contribution of [A] is neglected. However, a structural damping ratio of 0.002 is added.

Figure 7 shows the tuned aeroelastic response for r=6 i.e. σ =180 degrees for flat plate geometry. The unsteady aerodynamic coefficients are obtained at k_C = 1.0 for M=0.7. Calculations are done with a 155x41 grid for which the inlet and exit boundaries are located at one chord from the leading and trailing edges respectively. There are 55 points on the airfoil for this grid. The forcing frequency range investigated is limited to a small range around the 1st mode frequency. For the tuned cascade all the blades will have equal amplitudes. The amplitude of response is a function of the frequency ratio, ω / ω_o. Figure 7 shows the 1st generalized degree of freedom (q1) response obtained using linear theory and present LINFLX2D code. It can be seen that calculations from linear theory and from LINFLX2D are identical indicating that the coupling of LINFLX2D coefficients to ASTROP2 code for response calculations is also accurate.

Figure 8 shows the q1 response obtained for the C10 airfoil for M=0.7. Comparing the response of C10 with that of flat plate, it can be seen that the response has increased about 140%. This is due to high steady loading on the airfoil.

Figure 9 shows the q1 response obtained for the C10 airfoil for M=0.8. Comparing the response of C10 with that of flat plate, it can be seen that the response has increased to only about 68%. Observing from Fig 8 that the airfoil shape increased the response to about 140%, the decrease in the response in Fig 9 can be attributed to the presence of shock. However, the flow being transonic, it is planned to check the present calculations by running LINFLX2D for a different grid.

Concluding Remarks

The unsteady linearized Euler aerodynamic solver, LINFLX2D, has been successfully coupled with the ASTROP2 aeroelastic analysis code. The resulting code, ASTROP2-LE, is validated by comparing predictions from linear theory for flat plate geometry. Comparison was done for both flutter and forced response. Results were also presented for cascades in subsonic and transonic flow for a standard cascade

section known as C10 geometry. The following were observed during the study.

(1) The steady loading due to the airfoil shape, angle of attack destabilized the cascade for the Mach numbers considered.

(2) The steady loading due to the airfoil shape, angle of attack increased the blade response for subsonic flow and decreased response for transonic flow compared to that for a flat plate.

(3) An accurate steady solution called "low loss solution " is required for the unsteady solver LINFLX2D to work. This requires a considerable amount of computational time. This may be the biggest drawback of using this code in a design cycle.

(4) The success of getting an unsteady solution from LINFLX2D also depended on the grids used.

(5) It is to be noted that the number of LINFLX2D solutions required is directly related to number of strips. Care has to be taken in selecting the number of strips to reduce the number of calculations.

(6) For predicting the flutter boundary, calculations have to be done for a range of reduced frequencies. It is suggested that a LINFLX2D database be prepared for three or four reduced frequencies, and then interpolation be used for flutter calculations. These reduced frequency values can be selected by first running ASTROP2-LE with linear theory.

(6) The unsteady aerodynamic solution times varied from 20 minutes to 75 minutes on an SGI workstation. This is directly related to the number of iterations required for convergence. A solution for flat plate geometry took more time than for the C10 airfoil geometry.

(7) The LINFLX2D code can be used with any aeroelastic code that uses a typical section aeroelastic model as its basis.

References

(1)Reddy, et al, "A review of Recent Aeroelastic Analysis Methods for Propulsion at NASA Lewis Research Center", NASA TP 3406, December 1993.

(2)Whitehead, D.S., "Classical Two-Dimensional Methods", Chapter III in AGARD Manual on Aeroelasticity in Axial Flow in Turbomachines, Vol. 1, Unsteady Turbomachinery Aerodynamics, (ed. M. F. Platzer and F. O. Carta), AGARD-AG-298, Mar. 1987.

(3)Whitehead, D.S., "Force and Moment Coefficients for Vibrating Airfoils in Cascades", Aeronautical Research Council R&M 3254, Feb. 1960.

(4)Smith, S. N., "Discrete Frequency Sound Generation in Axial Flow Turbomachines," British Aeronautical Research Council, London, ARC R&M No. 3709, 1971.

(5)Rao, B. M. and Jones, W. P., "Unsteady Airloads on a Cascade of Staggered Blades in Subsonic Flow", Paper No. 32, AGARD-CP-177, September 1975.

(6)Adamczyk, J.J. and Goldstein, M.E., "Unsteady Flow in a Supersonic Cascade with Subsonic Leading-Edge Locus", ***AIAA Journal***, Vol. 16, No.12, pp. 1248-1254, Dec. 1978.

(7)Kaza, K. R. V. and Kielb, R. E., "Flutter and Response of a Mistuned Cascade in Incompressible Flow," ***AIAA Journal***, Vol. 20, No. 8, pp. 1120-1127, 1982.

(8)Kielb, R. E. and Kaza, K. R. V., "Aeroelastic Characteristics of a Cascade of Mistuned Blades in Subsonic and Supersonic Flows", ***ASME Journal of Vibration, Acoustics, Stress and Reliability of Design***, Vol. 105, pp. 425-433, Oct. 1983.

(9)Kaza, K. R. V.,Mehmed, O., Narayanan, G. V., and Murthy, D. V., "Analytical Flutter Investigation of a Composite Propfan Model", ***Journal of Aircraft***, Vol. 26, No. 8, Aug. 1989, pp. 772-780.

(10)Verdon, J. M., "Linearized Unsteady Aerodynamic Theory," Chapter II in AGARD Manual on Aeroelasticity in Axial Flow in Turbomachines, Vol. 1, Unsteady Turbomachinery Aerodynamics, (ed. M. F. Platzer and F. O. Carta), AGARD-AG-298, Mar. 1987.

(11)Verdon, J.M. and Caspar, J.R., "Development of a Linear Unsteady Aerodynamic Analysis for Finite Deflection Subsonic Cascades", ***AIAA Journal***, Vol. 20, pp. 1259-1267, 1982.

(12)Verdon, J.M. and Caspar, J.R.,"A Linearized Unsteady Aerodynamic Analysis for Transonic Cascades", ***Journal of Fluid Mechanics***, Vol. 149, pp. 403-429, 1984.

(13) Hoyniak, D., Verdon, J.V., "Steady and Linearized Unsteady Transonic Analyses of Turbomachinery Blade Rows", Unsteady Aerodynamics and Aeroelasticity of Turbomachines, Y. Tanida and M. Namba (editors), pp. 109-124,

1995.

(14)Smith, T. E. and Kadambi, J. R., "The Effect of Steady Aerodynamic loading on the Flutter Stability of Turbomachinery Blading", ***Journal of Turbomachinery***, Vol. 115, No. 1, pp. 167-174, 1993.

(15)Smith, T. E., "A Modal Aeroelastic Analysis Scheme for Turbomachinery Blading", NASA CR 187089, March 1991.

(16) Hall, K.C. and Clark, W.S., "Linearized Euler Predictions of Unsteady Aerodynamic Loads in Cascades", ***AIAA Journal***, vol. 31, No. 3, pp. 540-550, March 1993.

(17) Holmes, D.G. and Chuang, H.A., "2D Linearized Harmonic Euler Flow Analysis for Flutter and Forced Response", Unsteady Aerodynamic, Aeroacoustics, and Aeroelasticity of Turbomachines and Propellers, pages 213-230, Ed. Atassi, H.M, Springer-Verlag, New York, 1993

(18) Kahl, G. and Klose, A., "Computation of Time Linearized Transonic Flow in Oscillating Cascades", ASME Paper 93-GT-269, 38th IGT and Aeroengine Congress and Exposition, Cincinnati, Ohio, May 24-27, 1993.

(19) Verdon, J.V., Montgomery, M.D. and Kousen, K.A.," Development of a Linearized Unsteady Euler Analysis for Turbomachinery Blade Rows", NASA CR 4677, June 1995.

(20) Swafford, T.W., et al, "The Evolution of NPHASE: Euler/ Navier-Stokes Computations of Unsteady Two Dimensional Cascade Flow Fields", AIAA Paper 94-1834, 12th Applied Aerodynamics Conference, Colorado Springs, Colorado, June 20-23, 1994

(21)Reddy, T.S.R., Srivastava, R. and Mehmed, O., "Flutter and Forced Response Analysis of Cascades Using a Two Dimensional Linearized Euler Solver", to be published as NASA TM, Part of the material is presented as AIAA-98-3433, 34th Joint Propulsion Conference & Exhibit, July 13-15, 1998, Cleveland, OH

(22)Lane, F., "System Mode Shapes in the Flutter of Compressor Blade Rows," ***Journal of the Aeronautical Sciences***, Vol. 23, pp. 54-66, Jan. 1956.

(23) Srinivasan, A.V. and Fabunmi, J.A., "Cascade Flutter Analysis of Cantilevered Blades", Transactions of the ASME, **Journal of Engineering for Gas Turbines and Power**, Vol. 106, pp.34-43, January 1984.

(24) Narayanan, G.V. and Kaza, K.R.V., ASTROP2 Users Manual: A Program for Aeroelastic Stability Analysis of Propfans, Version 1.0, NASA TM 4304, August 1991.

(25) Reddy, T.S.R. and Lucero, J.M., ASTROP2 Users Manual: A Program for Aeroelastic Stability Analysis of Propfans, Version 2.0, NASA TM 107195, March 1996

ACKNOWLEDGMENTS

This work is supported by a grant from Machine Dynamics Branch under funding form Advanced Subsonic Technology Project and Smart Green Engine Project. George Stefko, John Rohde and Kestutis Civinskas are the technical monitors.

Table1: Aerodynamic Input Parameters at the Strips

Atmospheric pressure (psi)=13.1023; Speed of sound (fps)=1130.0

Strip Index	Stagger Angle (Degrees)	Chord Length (Inches)	Gap/Chord Ratio	Radius (Inches)	Strip width (inches)
1	45.0	3.145	1.0	5.407	0.1330
2	45.0	3.145	1.0	5.540	0.1335
3	45.0	3.145	1.0	5.674	0.1335
4	45.0	3.145	1.0	5.807	0.1335
5	45.0	3.145	1.0	5.941	0.1335
6	45.0	3.145	1.0	6.074	0.1335
7	45.0	3.145	1.0	6.208	0.1335
8	45.0	3.145	1.0	6.341	0.1335
9	45.0	3.145	1.0	6.475	0.1335
10	45.0	3.145	1.0	6.608	0.0669

Table 2: Mode shapes and frequencies used in the study

Table 2.1: Mode 1: natural frequency=81.376 HZ

Strip Index	Bending	Torsion
1	0.0	0.328
	0.0	0.444
3	0.0	0.584
4	0.0	0.627
5	0.0	0.693
6	0.0	0.742
7	0.0	0.793
8	0.0	0.889
9	0.0	0.937
10	0.0	1.000

Table 2.2: Mode 2: natural frequency=148.02 HZ

Strip Index	Bending	Torsion
1	-0.082	0.329
2	-0.087	0.446
3	-0.070	0.586
4	-0.058	0.630
5	-0.034	0.696
6	0.0	0.745
7	0.076	0.796
8	0.203	0.892
9	0.358	0.940
10	0.502	1.003

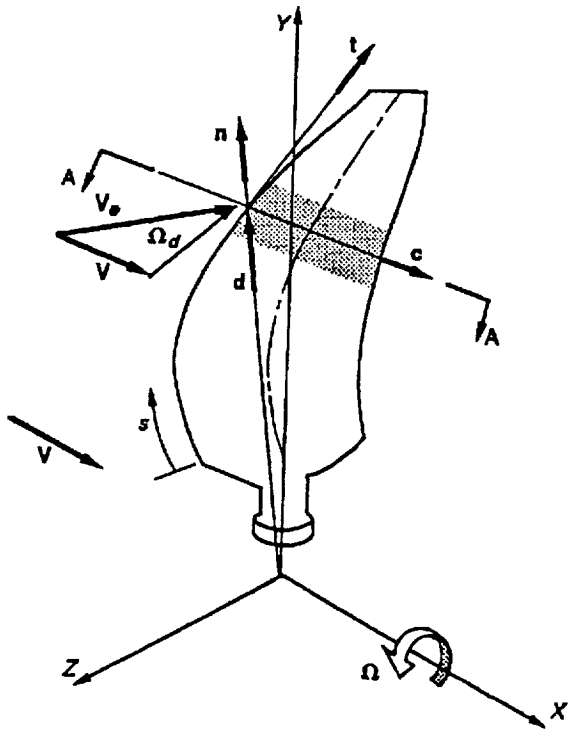

Figure 1a. : ASTROP2 coordinate system for a rotating blade

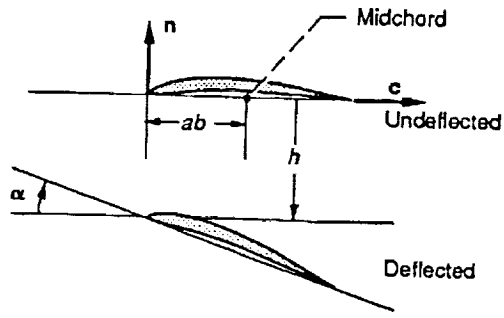

Figure 1b. : Section A-A showing rigid pitching (α) and plunging (h) motions for the strip (reference axis =leading edge)

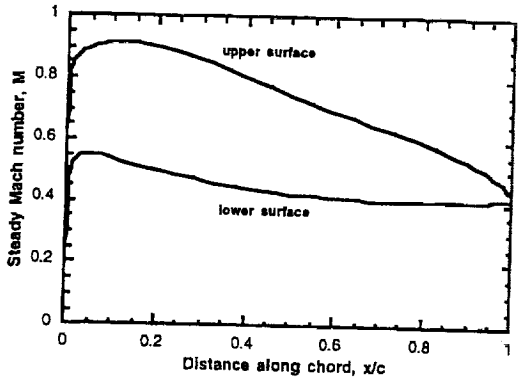

Fig2a.Steady Mach number distribution for a subsonic cascade, C10 airfoil, s/c=1.0, stagger=45 degrees, M=0.7, angle of attack = 10 degrees.

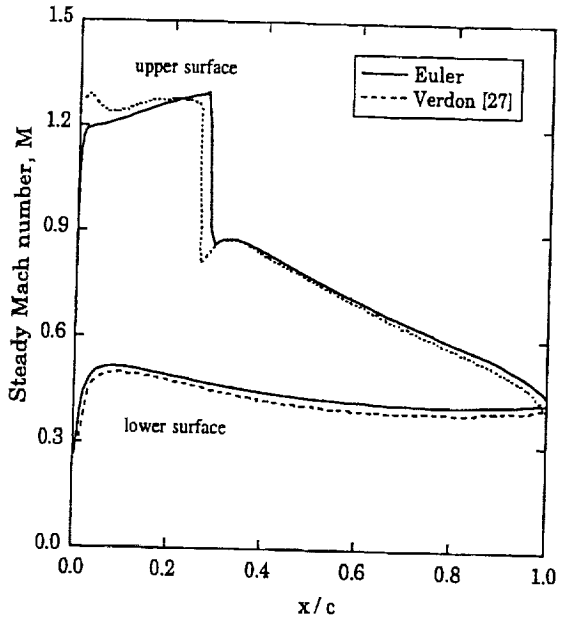

Figure 3a: Steady Mach number distribution for a transonic cascade; C10, $s/c = 1.0$, stagger $= 45°$, $M_\infty = 0.8$, $i = 13°$.

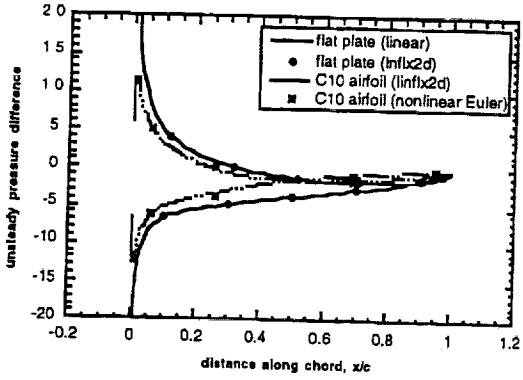

Figure 2b: Unsteady pressure difference distribution for a subsonic cascade, pitching about midchord, s/c=1.0,stagger=45 deg., M=0.7, kc=1.0,sigma=180 deg., alfa0=2 deg., I=0 for flat plate and I=10 for C10 airfoil

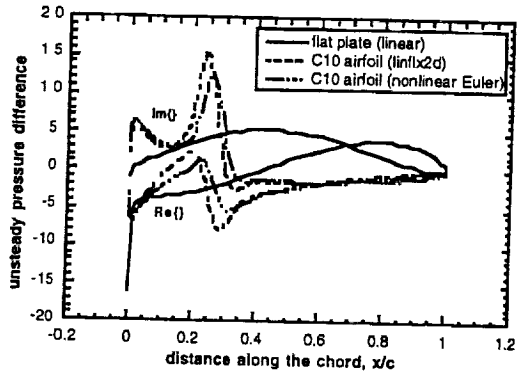

Figure 3b: Unsteady pressure difference distribution for a transonic cascade; C10 configuration, pitching about mid-chord

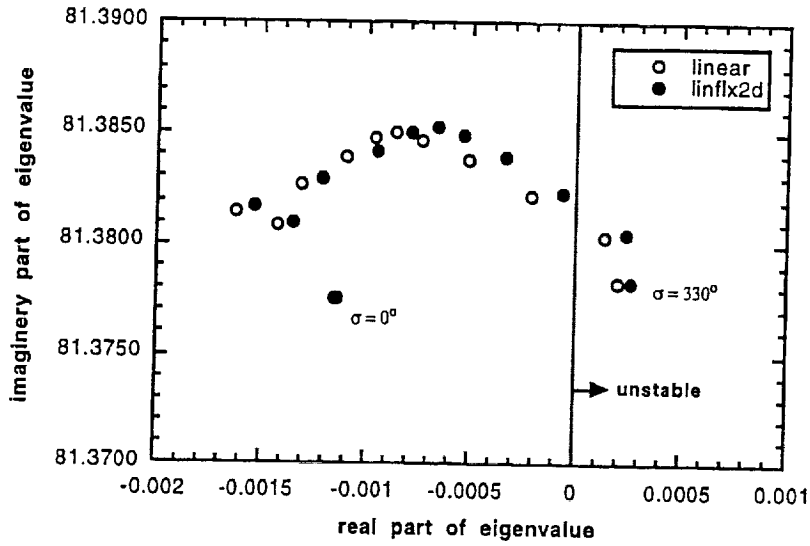

Figure 4. Root locus plot for 12 blade cascade, first mode, flat plate geometry, kb=0.1,structural damping=0.0,M=0.7

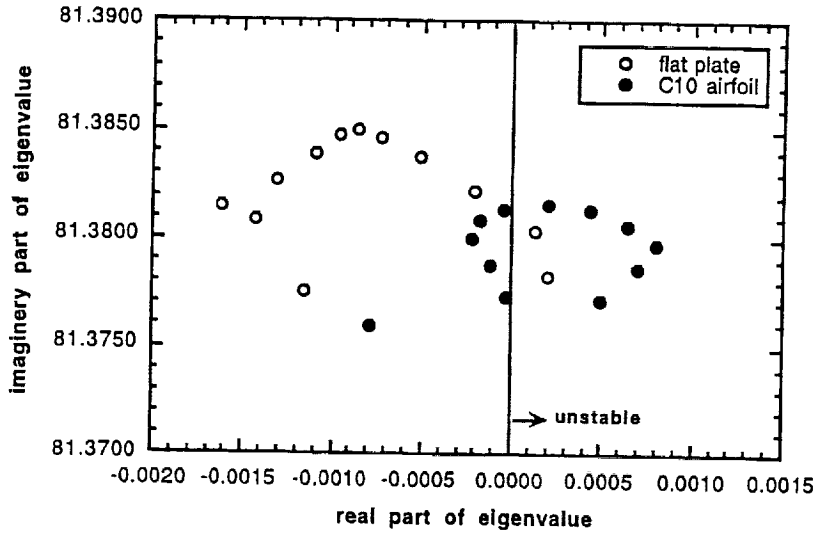

Figure 5. Root locus plot for 12 blade cascade, first mode, flat plate and C10 geometries, kb=0.1,structural damping=0.0,M=0.7

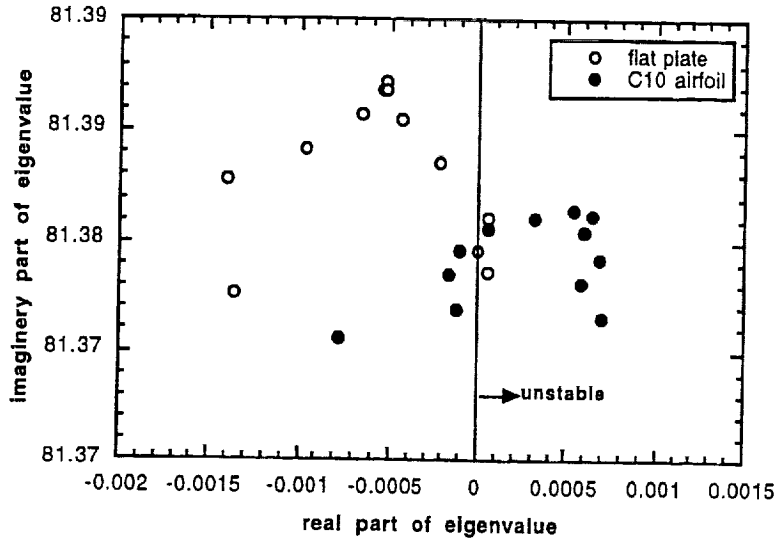

Figure 6. Root locus plot for 12 blade cascade, first mode, flat plate and C10 geometries, kb=0.1,structural damping=0.0,M=0.8

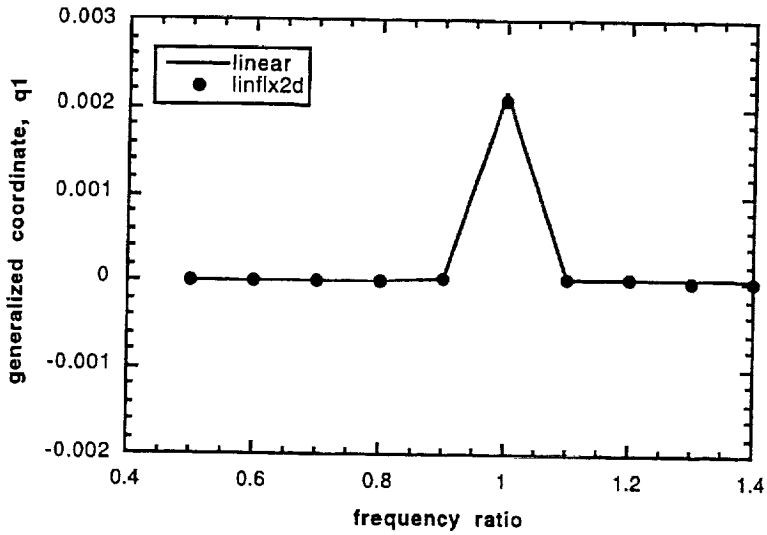

Figure 7. First mode response for a tuned cascade, flat plate geometry, structural damping =0.002, kb=0.5,N=12, flat plate geometry,M=0.7

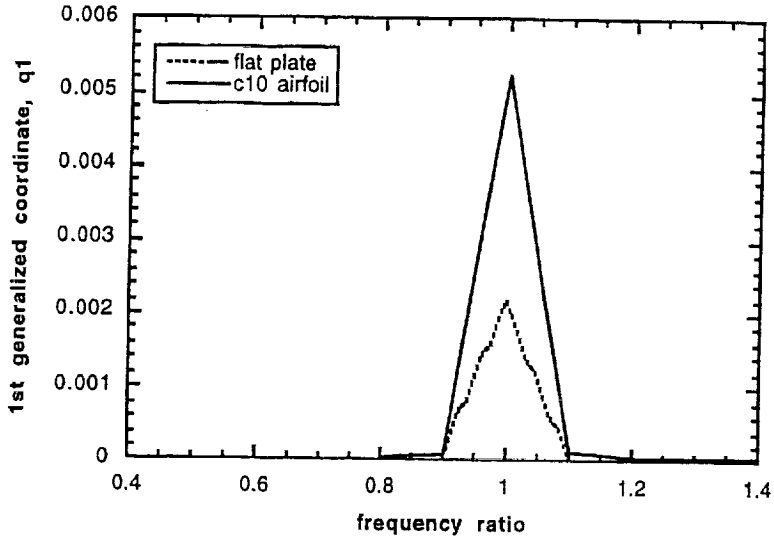

Figure 8. First mode response for a tuned cascade, flat plate geometry, structural damping =0.002, kb=0.5,N=12, flat plate and C10 geometries,M=0.7

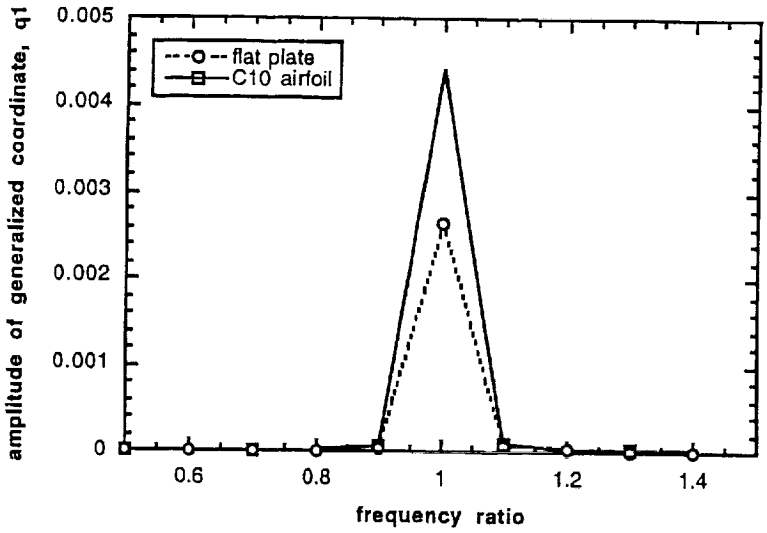

Figure 9. First mode response for a tuned cascade, flat plate geometry, structural damping =0.002, kb=0.5,N=12, flat plate and C10 geometries,M=0.8

AIAA-2000-3230

Development of a Turbomachinery Aeroelastic Code Based on a 3D Linearized Euler Solver

T. S. R. Reddy
Milind A. Bakhle
Theo G. Keith, Jr.

The University of Toledo
Toledo, Ohio

O. Mehmed

NASA Glenn Research Center
Cleveland, Ohio

36th AIAA/ASME/SAE/ASEE Joint Propulsion Conference and Exhibit
17-19 July 2000
Von Braun Civic Center
Huntsville, Alabama

AIAA-2000-3230

DEVELOPMENT OF A TURBOMACHINERY AEROELASTIC CODE BASED ON A 3D LINEARIZED EULER SOLVER

T.S.R. Reddy*
Milind A. Bakhle*
Theo G. Keith, Jr.+
The University of Toledo
Toledo, Ohio

O. Mehmed++
NASA Glenn Research Center
Cleveland, Ohio

Abstract

This paper describes the development of LINFLUX-AE, a turbomachinery aeroelastic code based on the linearized unsteady 3D Euler solver, LINFLUX. The steady solution, required by LINFLUX is obtained from the nonlinear Euler/Navier Stokes solver TURBO-AE. The paper briefly describes the salient features of TURBO-AE, LINFLUX and the details of the aeroelastic extension. The aeroelastic formulation is based on a modal approach. The unsteady aerodynamic forces required for flutter and forced response are obtained by running LINFLUX for each mode for each interblade phase angle and for a given frequency. An eigenvalue formulation is used for flutter analysis. The forced response is calculated from the modal summation of the generalized displacements. The NASA / GE Energy Efficient Engine (E- cubed) fan configuration is chosen as a test case and the results are compared with those obtained from TURBO-AE and ASTROP2.

Introduction

An overview of the aeroelastic analysis methods for turbomachines, Ref. 1, shows both time and frequency domain methods have been used to obtain unsteady aerodynamic forces and to solve the aeroelastic equations. It was noted that time domain methods require large computational times compared to frequency domain methods, and should only be used when non-linearity's are expected, and when the need justifies the cost. Two approaches were used in obtaining the unsteady aerodynamic forces using frequency domain methods. In the first approach, Ref.2, the unsteady aerodynamic equations are linearized about a *uniform* steady flow, thereby neglecting the effects of airfoil shape, incidence and thickness. The unsteady aerodynamic models developed in Refs. 3-6 based on this approach were used in Refs. 7-8 to study the flutter and forced response analysis of a compressor rotor and propfans. However, methods developed by this approach are restricted to shock-free flows through lightly loaded blade rows.

In the second approach, Ref. 9, the unsteady non-linear aerodynamic equations are linearized about the *non-uniform* steady flow, resulting in variable coefficient linear unsteady aerodynamic equations, which include the effects of steady aerodynamic loading due to airfoil shape, thickness and angle of attack. Following the second approach, steady and linear unsteady aerodynamic models have been developed based on the *potential equation,* Refs. 10-12. This unsteady aerodynamic model was integrated with a three dimensional structural model using strip theory in reference 13.

The formulation based on the potential equation requires corrections for entropy and rotational flow. The *Euler equations* can be used to correctly model rotational and entropy effects associated with strong shocks. Unsteady linearized Euler aerodynamic models that include the effect of steady aerodynamic loading were developed in Refs. 14-16. Recently, two and three-dimensional linearized Euler codes named respectively LINFLUX2D and LINFLUX were developed in references 17 and 18 under a NASA contract. These codes were based respectively on the non-linear Euler solver developed

* Member AIAA
+ University Distinguished Professor, Member AIAA
++ Research Engineer, Member AIAA

in Ref. 19 and Refs. 20-21. In Ref. 22, the unsteady aerodynamic calculations from LINFLUX2D were used with MISER (Ref. 7), an aeroelastic stability and response code based on a typical section structural model. Flutter and forced response calculations were presented for cascades in subsonic and transonic flow, and with and without mistuning. However, the aeroelastic formulation with MISER does not represent the actual behavior of a three dimensional structure. An ideal analysis will be to couple a three dimensional structural analysis with a three dimensional aerodynamic analysis.

The primary objective of the present study is to develop a 3D-aeroelastic code by coupling the 3-D linearized Euler analysis code, LINFLUX of Ref. 18, with a three-dimensional structural dynamics model. A modal approach will be used to do the flutter and response analysis. The resulting code will be called LINFLUX-AE to indicate the AeroElastic extension to LINFLUX code. Brief descriptions of the formulation and method of analysis are given in the next section, followed by results and concluding remarks.

Formulation

The aeroelastic formulation involves solutions from three models: a steady aerodynamic model, a linearized unsteady aerodynamic model and an aeroelastic model coupling the unsteady aerodynamic solution with the structural dynamic solution. The aerodynamic models and the aeroelastic formulation are described in this section.

Aerodynamic models

Non-linear Steady Euler Solver

The steady aerodynamic loading required for the linearized solver, LINFLUX, is obtained from the 3D Euler / Navier-Stokes solver TURBO-AE, Ref. 23. A very brief description of the TURBO code is presented in this section. Additional details regarding the code are available in Refs. 20-21 and 23.

The TURBO code was originally developed in Ref. 20 as an inviscid flow solver for modeling the flow through multistage turbomachinery. It has the capability to handle multiple blade rows with even or uneven blade count, stationary or rotating blade rows and blade rows at an angle of attack. Multiple blade passages are included in the calculation, when required. Additional developments were made in Ref. 21 to incorporate viscous terms into the model. The code can now be applied to model realistic turbomachinery configurations with flow phenomena such as shocks, vortices, separated flow, secondary flows, and shock and boundary layer interactions.

The code is based on a finite volume scheme. Flux vector splitting is used to evaluate the flux Jacobians on the left hand side of the governing equations and Roe's flux difference splitting is used to form a higher-order TVD scheme to evaluate the fluxes on the right hand side. Newton sub-iterations are used at each time step to maintain higher accuracy. A Baldwin-Lomax algebraic turbulence model is used in the code. Only the Euler option of the TURBO code is used in the present study.

Linear Unsteady Euler Solver, LINFLUX

To obtain the linearized unsteady Euler equations, Ref. 18, the dependent variables in the unsteady non-linear Euler equations are expanded in an asymptotic series of the form

$$U = U(\bar{x}) + u(x(\bar{x},t),t) + \text{higher order terms} \qquad (1)$$

Assuming the unsteady excitations are harmonic in time, and with the first order variable to be represented as complex valued, the above equation can be written as

$$U = U(\bar{x}) + \mathrm{Re}\{u(\bar{x})\exp(i\omega t)\} + \text{H.O.T.} \qquad (2)$$

Here, the term $U(\bar{x})$ is of order one and the second term is of the order ε.

Substituting the expansion of Eq. 2 in the non-linear unsteady Euler equations, and equating terms of like power in ε, and neglecting terms of second and higher order in ε, nonlinear steady equations and linear variable coefficient unsteady equations are obtained.

For harmonic blade motions with constant phase angle between adjacent blades (interblade phase angle), the values of interblade phase angle (σ) that can occur are given as (Ref. 24).

$$\sigma_r = 2\pi r / N \;;\; r = 0,1,2,\ldots\ldots, N-1 \qquad (3)$$

where N is the number of blades in the blade row. In a time domain approach with periodic boundary

conditions, the number of blade passages required to be modeled depends on the interblade phase angle, and small phase angles may require large number of blade passages to calculate the unsteady aerodynamic forces. However, with the linearized approach and the assumed harmonic variation in time, the periodic conditions are applied on a single extended blade passage region i.e., a region of angular pitch,

$$\theta = 2\pi / N \tag{4}$$

In solving the linearized unsteady equations, the dependent variables are regarded as pseudo-time dependent. This allows solutions to be determined using conventional time -marching algorithms to converge the steady and the complex amplitudes of the unsteady conservation variables to their steady state values. For more details, see reference 18.

Aeroelastic model

The aeroelastic equations of motion for each blade of the blade row of a turbomachine can be written as

$$[M]\{\ddot{X}\} + [K]\{X\} = \{P(X),t)\} + \{F(t)\} \tag{5}$$

where [M] is the mass matrix, [K] is the stiffness matrix that includes the effects of rotation (centrifugal stiffening and softening), {X} is the vector of blade deflections at the finite element grid points, {P(X),t} is aerodynamic force vector due to blade vibration that may cause instability, and {F(t)} is the aerodynamic force vector due to gust leading to fatigue failures due to forced response.

A modal formulation is used to proceed further. The starting point is to obtain a free vibration solution of the blades giving generalized masses, natural frequencies, and mode shapes. This solution can be obtained either by using commercial finite element codes or by writing one's own analysis solver. The general vibratory motion then can be expressed as a superposition of the contributions of the normal modes, $[\phi] = [\phi_1, \phi_2, ..., \phi_{NM}]$, as

$$\{X\} = [\phi]^T \{q\} = \sum_{i=1}^{i=NM} \phi_i q_i \tag{6}$$

where $\{q\}$ is the generalized displacement, and NM is the number of normal modes to be used in the analysis. Substituting Eq. 6 in Eq. 5, and post multiplying the result by $[\Phi]^T$, the equations of motion for the s^{th} blade can be written as

$$[M_s]\{\ddot{q}_s\} + [K_s]\{q_s\} = [A_s]\{q_s\} + \{AD_s\} \tag{7.1}$$

where

$$[M_s] = [\phi]^T [M][\phi];$$

$$[K_s] = [\phi]^T [K][\phi]; \tag{7.2}$$

$$[A_s] = [\phi]^T \{P(X),t\};$$

$$\{AD_s\} = [\phi]^T \{F(t)\}$$

where $[M_s]$ and $[K_s]$ are generalized mass and stiffness matrices, which are diagonal, $\{q_s\}$ is the generalized displacement vector, and $[A_s]$ is the motion *dependent* generalized aerodynamic load matrix, and $\{AD_s\}$ is the motion *independent* generalized aerodynamic load vector. The motion dependent forces cause flutter, and motion independent forces cause forced response (forced vibration). The matrices $[M_s]$, $[K_s]$, and $[A_s]$ are of NM x NM size, $\{q_s\}$ and $\{AD_s\}$ are of NM x 1 size.

For a tuned cascade (or rotor), in which all the blades are identical, the aeroelastic modes consist of individual blades vibrating with equal amplitudes with a fixed interblade phase angle between adjacent blades. Hence, the motion of the sth blade in rth interblade phase angle mode can be written as

$$\{q_s\} = \{q_{os}\} e^{i\omega t} = \{q_{ar}\} e^{i\omega t} e^{i\sigma_r s} \tag{8}$$

where σ_r is given by Eq. 3.

Thus the equations of motion for the blade, Eq. 7.1 becomes

$$-\omega^2 [M_s]\{q_{ar}\} e^{i(\omega t + \sigma_r s)} + [K_s]\{q_{ar}\} e^{i(\omega t + \sigma_r s)} = [A_r]\{q_{ar}\} e^{i(\omega t + \sigma_r s)} + \{AD_r\} e^{i(\omega t + \sigma_r s)} \tag{9}$$

Since the blades are identical, the same equation is obtained for each blade. Thus, no additional information can be obtained by assembling the equations for all the blades on the disk. Instead, equation (9) can be solved for *N* different values of the interblade phase angle given by equation (3).

Dropping the subscript s, since each blade is identical, and canceling out the exponential terms, Eq. 9 can be written as

$$-\omega^2 [M] \{Y\} + [K]\{Y\} - [A_r]\{Y\} = \{AD_r\} \quad (10)$$

where {Y} is same as $\{q_{ar}\}$.

Calculation of Elements of $[M_s]$, $[K_s]$ *and* $[\phi]$

The elements of $[M_s]$, $[K_s]$ and $[\phi]$ are given by the free vibration analysis using a commercial code like ANSYS/ NASTRAN or by writing own analysis program. The matrices $[M_s]$ and $[K_s]$ are diagonal. The elements of $[M_s]$ and $[K_s]$ are related as

$$K_{ii} = M_{ii}\,\omega_{ii}^2 \quad (11)$$

where ω_{ii} is the natural frequency of the i^{th} mode. It is to be noted that usually the mode shapes are mass normaized giving $M_{ii} = 1.0$.

Calculation of elements of $[A_r]$ and $\{AD_r\}$

The elements of $[A_r]$ and $\{AD_r\}$ are obtained from LINFLUX code. The code is run for a given frequency and interblade phase angle for a given mode. The output is the real and imaginary components of unsteady pressures. This is repeated for NM modes of vibration. In the case of forced response for a gust, the code is run only once for the unsteady excitation.

The mode shape values are interpolated onto the aerogrid before running LINLFUX as follows: At each CFD grid point on the blade surface, the distance to the nearest three finite-element grid points is calculated. Then, the modal deflections at these three nearest neighbors are used in a bi-linear interpolation scheme to calculate the interpolated value of the modal deflection at that CFD grid point. This is done considering the blade undeflected position as the reference position. The interpolated modal deflections $\bar{\delta}$ are stored and are used by LINFLUX.

<u>Calculation of elements of</u> $\{AD_r\}$

The elements of {AD} are due to the external unsteady disturbances coming on to the blade. These may be due to entropic, vortical and wake interactions. These disturbances are independent of the blade vibratory motion, and therefore contribute only to the forced response aspect of the aeroelastic problem. The LINFLUX solver can calculate the unsteady pressures due to these excitations for a given interblade phase angle, r. Let p be the unsteady pressure due to these excitations on the blade surface. Then the elements of $\{AD_r\}$ are given by

$$\{AD_r\} = \int p_r \, d\bar{A}.\bar{\delta}_i \quad (12)$$

where δ_i is the i^{th} mode shape.

<u>Calculation of elements of</u> $[A_r]$

The elements of $[A_r]$ are due to the vibration of the blade in a given mode. It requires moving the aerogrid in the given mode in the aerodynamic calculations, and a given frequency, and calculating the unsteady aerodynamic forces. The LINFLUX solver can accept the modal values at each grid point and can modify the grid as per the modal values. Once the unsteady aerodynamic pressures are calculated, the elements of {A} are given as

$$A_{rij} = \int \bar{\delta}_i . d\bar{A}\, p_{rj} \quad (13)$$

where p_{rj} is the unsteady pressure due to blade vibration in j^{th} mode for the rth interblade phase angle, $\bar{\delta}_i$ is the i^{th} modal deflection, and dA is the elemental area.

When running LINFLUX the pressure is usually output as a non-dimensional quantity, which is multiplied by $(\rho * a_\infty^2)$ to get the actual pressure values, where ρ is the reference air density and a_∞ is the reference speed of sound. In calculating area and modal values, attention should be given to the non-dimensionlization to length scaling. If L is the reference length used for scaling the geometry and the modal values, the final A_{ij} have to be multiplied by L**3 (L for modal values and L**2 for area). It should also be noted that the modal values (mode shape) when input to LINFLUX should be divided by the reference length.

Stability calculation

Aerodynamic work approach

A work-per-cycle approach can be used to determine aeroelastic (flutter) stability. Using this approach, the motion of the blade is prescribed to be a harmonic vibration in a normal mode with a specified frequency. The vibration frequency is typically the natural frequency for the mode of interest, but some other frequency can also be used. The aerodynamic forces acting on the vibrating blade and the work done by these forces on the vibrating blade during a cycle of vibration are calculated. If work is being done *on* the blade by the aerodynamic forces, the blade is dynamically unstable, since it will result in extraction of energy from the flow, leading to an increase in amplitude of oscillation of the blade. Note that coupled mode flutter cannot be modeled with this approach.

To determine aeroelastic stability using the work-per-cycle approach, the blade motion is specified to be harmonic:

$$q(t) = q_0 \sin(\omega t) \qquad (14)$$

where q_o is the amplitude of motion and ω is the vibration frequency.

The work-per-cycle, W, done on the blade is calculated as:

$$W = \oint \int_S p d\bar{A}.(\partial \bar{X} / \partial t) dt \qquad (15.1)$$

or,

$$W = \oint \int_S p d\bar{A}.\delta q_0 \omega \cos(\omega t) dt \qquad (15.2)$$

where, $p = p(x,y,z,t)$ is the unsteady pressure on the blade surface due to blade vibration, $\vec{A}$ is the blade surface area vector pointing *into* the blade surface, $\int_S$ is the integral over the blade surface, $\oint$ is the integral over one cycle of blade vibration. The equation for work per cycle using the linearized unsteady aerodynamic equations is given in Ref. 18.

The work-per-cycle is an indicator of aeroelastic stability. The blade is dynamically unstable if the work done *on* the blade during a cycle of blade vibration is positive. In other words, when W < 0 energy is dissipated by the blade and the system is stable, but when W > 0, energy is gained by the blade and it is unstable.

Eigenvalue approach

An eigenvalue approach allows one to investigate coupled mode flutter. The flutter frequencies and flutter modes are calculated rather than assumed as in aerodynamic work approach. For a stability calculation (flutter), the motion-independent forces $\{AD_r\}$ are set to zero, and Eq. (10) can be written as

$$-\omega^2 [M] \{Y\} + [K]\{Y\} - [A_r] \{Y\} = \{0\} \qquad (16)$$

Dividing Eq. 16 with an assumed frequency, ω_o^2

$$-(\omega/\omega_o)^2 [M]\{Y\} + [[K]-[A_r]]\{Y\} / \omega_o^2 = \{0\} \qquad (17)$$

Rearranging, the equations can be written in the standard eigenvalue problem as:

$$[[P_r] - \gamma[Q]]\{Y_r\} = \{0\} \qquad (18)$$

where

$$[P_r] = [[K] - [A_r]]/\omega_o^2 \qquad (19)$$

$$[Q_r] = [M] \qquad (20)$$

and

$$\gamma = (\omega/\omega_o)^2 \qquad (21)$$

The solution of the above eigenvalue problem results in NM complex eigenvalues of the form

$$i\frac{\omega}{\omega_o} = i\sqrt{\gamma} = \bar{\mu} + i\bar{\nu} \qquad (22)$$

The real part of the eigenvalue ($\bar{\mu}$) represents the damping ratio, and the imaginary part ($\bar{\nu}$) represents the damped frequency; flutter occurs if $\bar{\mu} \geq 0$ for any of the eigenvalues.

For the tuned cascade, the stability of each phase angle mode is examined separately. The interblade phase angle is fixed at one of the values given by equation (3), and the NM x NM eigenvalue problem is solved. The value of interblade phase angle is then

changed, and the procedure is repeated for each of the N permissible values. The critical phase angle is identified as the one, which results in the lowest flutter speed.

Response Calculation:

The aeroelastic response of the blades induced by wakes is calculated from equation (10) as

$$\{Y_r\} = \left[[P_r] - \lambda[Q]\right]^{-1}\{AD_r\} \qquad (23)$$

The amplitude of the blade, {X}, is obtained by summing contributions of {Y} from all the modes.

Results

Results are presented for selected three-dimensional geometry's in this section. Results presented here are meant to demonstrate the state of development of the code. The procedure to do a complete aeroelastic analysis is shown in Fig.1. The procedure consists of running six codes, (I) a free vibration analysis and the corresponding processing code, RDVIB, (II) TURBO-AE, (III) INTERFACE, (IV) a PRE-processor, (V) LINFLUX, and (VI) a POST-processor. The function of each program is explained below in six steps and shown in table 1. In step 1 a vibration analysis is done for the blade. The output is structural gird coordinates, generalized masses, natural frequencies, and mode shapes. RDVIB reads this output and writes in a format required by the pre-processor. In step 2, a steady aerodynamic solution is obtained from TURBO-AE for the blade. The steady aerodynamic solution is written as a database. Step 3 consists of running the INTERFACE program to rewrite the steady data base to the format required by LINFLUX. In step 4 the pre-processor is run. This will interpolate modal values at the structural grid onto the aerogrid, for all the modes. In step 5, LINFLUX is executed for the mode of interest and frequency. At this stage LINFLUX also calculates work per cycle for the mode of interest. In step 6 the post processor is run, to calculate the generalized forces, to calculate flutter using the eigenvalue approach and to calculate forced response amplitudes.

Two examples are given below to show that the whole process is working as intended. In the present paper, the verification of unsteady pressures, and eigenvalue calculations is given. The unsteady pressures calculated using LINFLUX code are compared with those obtained from TURBO-AE and LINSUB codes. TURBO-AE is a three-dimensional Euler aeroelastic code developed in Ref.23, and LINSUB is a two-dimensional unsteady cascade aerodynamic code based on linear unsteady aerodynamic theory of Smith, Ref. 3. The eigenvalue calculations are compared with those obtained from ASTROP2 code of Ref. 8. The ASTROP2 code uses strip theory to integrate two-dimensional aerodynamic forces on to a three dimensional structure. The aerodynamic forces are calculated about leading edge, using linear unsteady aerodynamic theory of Ref. 4. It uses eigenvalue approach to calculate flutter stability. The verification of forced response amplitudes will be presented in a subsequent paper.

Helical Fan

The helical fan configuration consists of a rotor with twisted flat plate blades enclosed in a cylindrical duct with no tip gap. This configuration was developed by researchers to provide a relatively simple test case for comparison with two-dimensional analyses. Note that there is no experimental data available for this configuration.

The parameters for this configuration are such that the mid-span location corresponds to a flat plate cascade with a stagger angle of 45 degrees, unit gap-to-chord ratio, operating in a uniform mean flow at a Mach number of 0.7 parallel to the blades. The rotor has 24 blades with a hub/tip ratio of 0.8. The radius at the hub is 8.619 cm (3.395 inches) and the radius at the tip is 10.775 cm (4.244 inches). The inlet flow (axial) Mach number used in this calculation is 0.495, and the rotation speed of the fan is 16,962.4 rpm, which results in a relative Mach number of approximately 0.7 at the mid span section.

The grid used for the calculations is 141x11x41 in each blade passage. On each blade surface, 81 points are located in the chordwise direction, 11 points in the spanwise direction, and 41 points in blade to blade direction. The inlet and exit boundaries are located at an axial distance of approximately 0.7 chord lengths from the blade leading and trailing edges. A steady solution is obtained first with TURBO-AE solver (step 2). Program INTERFACE is run to convert the steady aerodynamic solution data to the form required by LINFLUX (step 3). Next unsteady pressures are calculated for harmonic blade vibration in plunging and pitching modes. Mode shapes (step 1) are prescribed (i.e. no

structural analysis is done) such that the amplitude of vibration does not vary along the span. This choice of mode shapes is meant to reduce the three dimensionality of the unsteady flow field for ease of comparison with two-dimensional analyses.

LINFLUX can be run by an input choice, iflut=1, by having these prescribed mode shapes *internally* calculated. However, the purpose of this effort is to run for arbitrary mode shapes that are calculated *outside* LINFLUX and to see that they are correctly read by LINFLUX. To check this, the mode shapes are obtained by running LINFLUX with iflut=1 and are written on unit 3. PRE is then run to interpolate the mode shapes onto the aerogrid. But for this case this will not change the modal values at the aerogrid points since the modal values are obtained form LINFLUX to start with. So actually step 4 is not required for this example. After running PRE the interpolated mode shapes are written on unit 27. Now LINFLUX is run with iflut =2, which reads the externally supplied mode shape values at aero-grid points. LINFLUX is run for unsteady pressures and compared with those obtained with iflut=1 and published results.

Figures 2 and 3 show the unsteady pressures at mid span obtained for a reduced frequency, ω, of 1.0($\omega = \omega_0 L/U = \omega_0 L/a_\infty M_r = \bar{\omega}/M_r$, where $\bar{\omega} = \omega_0 L/a_\infty$, and L is the reference length. It should be noted that $\bar{\omega}$ is the input to LINFLUX.). For the present calculations the value of speed of sound, a_∞, is assumed as 13707 in/sec, reference length is the chord which is 1.0 inch giving, a value of 1527 cycles/sec for the assumed frequency ω_0. Figure 2 is for plunging motion and Fig 3 is for pitching motion about leading edge. Fig 2.1 is for zero phase angle, fig. 2.2 is for 180 degrees phase angle. Figures for 3.1 and 3.2 show the unsteady pressure distributions for pitching motion for zero and 90 degrees phase angle respectively. The pressures are compared with those obtained from LINSUB code based on Smith theory, Ref. 3. To compare with LINSUB results, the unsteady pressure output from LINFLUX is divided by square of the Mach number times the amplitude of oscillation. The pressure distribution predictions from LINFLUX show excellent agreement with those from LINSUB.

Next the unsteady pressure distributions from LINFLUX are compared with those obtained from TURBO-AE in figures 4 and 5. Figure 4 is for plunging motion for zero and 180 degree phase angles and figure 5 is for pitching motion for zero and 90 degrees phase angles. Again, excellent agreement is seen between the predictions.

Table 2 shows the work-per-cycle calculations for this case, and comparison with TURBO-AE, Ref. 23. The work per cycle for plunging motion shows excellent agreement, however, the calculations for pitching motion show a lot of difference. This may be due to an error in normalization, since unsteady pressures shown earlier agreed well for this case. Some of these results were also reported in Ref. 18. They are included here for completeness, and to show that the present authors successfully ran LINFLUX code as intended, and for externally calculated mode shapes.

Next, the calculated unsteady pressures are used by POST to calculate generalized forces and eigenvalues. The generalized forces are calculated using the prescribed mode shape used for the unsteady aerodynamic pressure calculation. To validate the eigenvalue calculations, the present results are compared with those obtained from the ASTROP2 code. As mentioned before, the ASTROP2 code uses strip theory to integrate two-dimensional aerodynamic forces on to a three dimensional structure. The aerodynamic forces are calculated about leading edge, using theory of Ref. 4. It uses eigenvalue approach to calculate stability. As unsteady pressures are already compared above with Smith theory, this aspect will give validation to the calculation of generalized forces and eigenvalues. Table 3 shows the eigenvalues obtained by the present post processor and the ASTROP2 code for an assumed frequency of $\bar{\omega}$ = 0.7 and for σ = 0 degrees. They show excellent correlation. As expected, the eigenvalues indicate that the blades are stable, which was also indicted by the work per cycle approach in TURBO-AE and LINFLUX programs. This validates the routines in the post-processor.

Energy Efficient Engine, E3

In this section, an example is considered where the mode shapes are *not* prescribed as for helical fan but obtained from a modal analysis. The configuration selected is derived from the Energy Efficient Engine (E-cubed) fan rotor. The E-cubed program was established by GE Aircraft Engines under NASA sponsorship in the 1980's to demonstrate component technologies necessary to achieve higher efficiencies and reduce environmental effects in future subsonic

turbofan engines. Details regarding design and performance tests have been presented in Ref. 25.

The fan rotor has 32 blades with a tip diameter, D, of 210.8 cm (83 inches). The inlet Mach number is 0.5. The fan is rotating at a speed of 2727 rpm. The CFD grid is a simple sheared grid of size 43x15x11 with 15 points on the blade surface in both the chordwise and spanwise directions. It is assumed that the tip gap is zero. The finite-element structural dynamics data is for a structural grid with 224 points.

First a structural dynamic solution is obtained giving the modal frequencies and mode shapes. (step 1). The first mode is predominately bending with a frequency of 72.4 Hz, and the second mode is predominately torsion with a frequency of 163.8 Hz.

A steady solution is obtained for this configuration using TURBO-AE. (step 2). The steady data base is processed through INTERFACE to get formatted data for LINFLUX (step 3). Then PRE is run to interpolate the modal values onto the aerogrid (step 4). The interpolated modal values are verified by plotting the deflected blade shape (not included here) and by manually checking the tip displacement values. Overall, the interpolated deflections matched the original deflections except for slight differences in the blade tip region.

The unsteady aerodynamic solutions are then performed using LINFLUX. LINFLUX is run for a frequency of oscillation equal to the first mode (step 5). The non-dimensional frequency $\overline{\omega} = \omega D / a_\infty$ input to LINFLUX is 2.732. Figures 6.1 through 6.4 show the unsteady pressures plotted for mid span for zero, 90, 180 and 270 degree phase angles. They are compared with TURBO-AE results. The TURBO-AE results are obtained using 100 steps per cycle. It can be seen that there is considerable difference between the two results, even though the trends are same. The difference is attributed to the fact that LINFLUX requires a very good steady solution, especially near leading edge, to get a comparable solution with TURBO-AE predictions.

Figure 7.1 and 7.2 shows the unsteady pressures compared for the second mode. The non-dimensional frequency $\overline{\omega} = \omega D / a_\infty$ input to LINFLUX is 4.183. It is to be noted that the value of the frequency parameter calculated with the second frequency is 6.18263. However, with this value the unsteady solution could not be obtained with LINFLUX. Therefore, the value is reduced to 4.183, where an unsteady solution could be obtained for σ =0 and 270 degrees. Again, even for this value of $\overline{\omega}$, solution could not be obtained for σ = 90° and 180°. There may be two reasons for this behavior: (1) the steady solution is not sufficiently converged for LINFLUX run, (2) there is an inherent problem with LINFLUX that requires experience with CFL numbers, grid etc.

Table 4 shows the work per cycle calculations from LINFLUX compared to TURBO-AE results. Both show a considerable difference. This is believed to be due to the coarse grid used in the calculations, and further calculations should be done with finer grid for this fan. Table 5 shows the eigenvalues calculated for this fan from POST and ASTROP2 for $\overline{\omega}$ = 4.183 or ω_o = 111 Hz and for σ = 0 degrees. There is some difference which is expected as the linear unsteady aerodynamic analysis in ASTROP2 neglects the effect of steady loading on flutter.

Concluding Remarks

The status of a turboamchinery aeroelastic code LINFLUX-AE is presented. The code is based on running four codes, one for steady aerodynamic solution, a linearized unsteady aerodynamic solution and for flutter and response calculations. Other modules required for connecting these solutions are developed and verified. These include a preprocessor to read structural vibration data, an interface for reading steady aerodynamic solution data and routine to interpolate mode shapes on to aero-grid, and routines for calculating eigenvalues and response amplitudes.

The code is verified by running for two three-dimensional geometry fans. A helical fan with flat plate airfoils provided comparison with published results and a E-cubed fan providing calculation for a realistic fan.

It was noted that for the helical fan with flat plate geometry, the unsteady pressures calculated from LINFLUX agreed well with LINSUB and TURBO-AE. However, the work per cycle calculations for pitching motion are not identical between LINFLUX and TURBO-AE. The flutter eigenvalues for an idealized flutter analysis showed the eigenvalues from LINFLUX-AE are close of those obtained from ASTROP2.

For the E-cubed fan geometry, the unsteady pressures from LINFLUX and TURBO-AE showed considerable difference. This may be due to the fact

that the steady solution obtained from TURBO-AE is not a sufficiently accurate solution for LINFLUX code. This affected the work per cycle calculations also. In addition, unsteady solutions could not be obtained for some phase angles and some frequencies with LINFLUX. It is suggested that all the calculations for E-cubed fan be redone with a steady solution obtained with a fine grid. Further runs with some more 3D geometry's and validation of forced response calculations are planned for future.

Acknowledgements

This work was supported by a grant from the NASA Glenn Research Center, Structural Mechanics and Dynamics Branch (George Stefko, manager) with funding from the Turbomachinery and Combustion Technology Project. Robert Corrigan is the program manager.

References

(1) Reddy, et al, "A review of Recent Aeroelastic Analysis Methods for Propulsion at NASA Lewis Research Center", NASA TP 3406, December 1993.

(2) Whitehead, D.S., "Classical Two-Dimensional Methods", Chapter III in AGARD Manual on Aeroelasticity in Axial Flow in Turbomachines, Vol. 1, Unsteady Turbomachinery Aerodynamics, (ed. M. F. Platzer and F. O. Carta), AGARD-AG-298, Mar. 1987.

(3) Smith, S. N., "Discrete Frequency Sound Generation in Axial Flow Turbomachines," British Aeronautical Research Council, London, ARC R&M No. 3709, 1971.

(4) Rao, B. M. and Jones, W. P., "Unsteady Airloads on a Cascade of Staggered Blades in Subsonic Flow", Paper No. 32, AGARD-CP-177, September 1975.

(5) Adamczyk, J.J. and Goldstein, M.E., "Unsteady Flow in a Supersonic Cascade with Subsonic Leading-Edge Locus", ***AIAA Journal***, Vol. 16, No.12, pp. 1248-1254, Dec. 1978.

(6) Williams, M.H., " An Unsteady Lifting Surface Method for Single Rotation Propellers", NASA CR 4302, 1990.

(7) Kaza, K. R. V. and Kielb, R. E., "Flutter and Response of a Mistuned Cascade in Incompressible Flow," ***AIAA Journal***, Vol. 20, No. 8, pp. 1120-1127, 1982.

(8) Kaza, K. R. V., Mehmed, O., Narayanan, G. V., and Murthy, D. V., "Analytical Flutter Investigation of a Composite Propfan Model", ***Journal of Aircraft***, Vol. 26, No. 8, Aug. 1989, pp. 772-780.

(9) Verdon, J. M., "Linearized Unsteady Aerodynamic Theory," Chapter II in AGARD Manual on Aeroelasticity in Axial Flow in Turbomachines, Vol. 1, Unsteady Turbomachinery Aerodynamics, (ed. M. F. Platzer and F. O. Carta), AGARD-AG-298, Mar. 1987.

(10) Verdon, J.M. and Caspar, J.R.,"A Linearized Unsteady Aerodynamic Analysis for Transonic Cascades", ***Journal of Fluid Mechanics***, Vol. 149, pp. 403-429, 1984.

(11) Verdon, J.M. and Hall, K.C., "Development of a Linearized Unsteady Aerodynamic Analysis for Cascade Gust Response Predictions", NASA CR 4308, 1990.

(12) Hoyniak, D., Verdon, J.M., "Steady and Linearized Unsteady Transonic Analyses of Turbomachinery Blade Rows", Unsteady Aerodynamics and Aeroelasticity of Turbomachines, Y. Tanida and M. Namba (editors), pp. 109-124, 1995.

(13) Smith, T. E., "A Modal Aeroelastic Analysis Scheme for Turbomachinery Blading", NASA CR 187089, March 1991.

(14) Hall, K.C. Clark, W.S. and Lorence, C.B., "A Linearized Euler Analysis of Unsteady Transonic Flows in Turbomachinery", ASME Paper 93-GT-94, 38th IGT and Aeroengine Congress and Exposition, Cincinnati, Ohio, May 24-27, 1993.

(15) Holmes, D.G. and Chuang, H.A., "2D Linearized Harmonic Euler Flow Analysis for Flutter and Forced Response", Unsteady Aerodynamic, Aeroacoustics, and Aeroelasticity of Turbomachines and Propellers, pages 213-230, Ed. Atassi, H.M, Springer-Verlag, New York, 1993

(16) Kahl, G. and Klose, A., "Computation of Time Linearized Transonic Flow in Oscillating Cascades", ASME Paper 93-GT-269, 38th IGT and Aeroengine Congress and Exposition, Cincinnati, Ohio, May 24-27, 1993.

(17) Verdon, J.M., Montgomery, M.D. and Kousen,

K.A.," Development of a Linearized Unsteady Euler Analysis for Turbomachinery Blade Rows", NASA CR 4677, June 1995.

(18) Montogomery, M.D. and Verdon, J.M., "A Three-Dimensional Linearized Unsteady Euler Analysis for Turbomachinery Blade Rows", NASA CR 4770, March 1997.

(19) Swafford, T.W., et al, "The Evolution of NPHASE: Euler/ Navier-Stokes Computations of Unsteady Two Dimensional Cascade Flow Fields", AIAA Paper 94-1834, 12th Applied Aerodynamics Conference, Colorado Springs, Colorado, June 20-23, 1994

(20) Janus, J.M., "Advanced 3-D CFD Algorithm for Turbomachinery", Ph.D. Dissertation, Mississippi State University, Mississippi, 1989.

(21) Chen, J.P., "Unsteady Three-Dimensional Thin-Layer Navier-Stokes Solutions for Turbomachinery in Transonic Flow", Ph.D. Dissertation, Mississippi State University, Mississippi, 1991.

(22) Reddy, T.S.R., Srivastava, R. and Mehmed, O., "Flutter and Forced Response Analysis of Cascades Using a Two Dimensional Linearized Euler Solver", NASA TM- 1999- 209633, November 1999.

(23) Bakhle, M.A., Srivastava, R., Keith, Jr., T, Stefko, G.L., A 3D Euler / Navier-Stokes Aeroelastic Code for Propulsion Applications, AIAA 97-2749, 33rd AIAA /ASME / ASME/ SAE ASEE Joint Propulsion Conference & Exhibit, July 6-9, 1997, Seattle, WA

(24) Lane, F., "System Mode Shapes in the Flutter of Compressor Blade Rows," ***Journal of the Aeronautical Sciences***, Vol. 23, pp. 54-66, Jan. 1956.

(25) Sullivan, T.J., and Hager, R.D., "The Aerodynamic Design and Performance of the General Electric / NASA E-cubed Fan", AIAA Paper 83-1160, 1983.

Table 1: LINFLUX-AE modules and their function

steps	program name	function
1	RDVIB	(1) do free vibration analysis. At present done outside this program through ANSYS, NASTRAN etc. (2) read vibration analysis output file and rotate the grid and mode shapes to aero-grid coordinate system, write on UNIT 3
2	TURBO-AE	do steady aerodynamic analysis
3	INTERFACE	convert TURBO-AE output to data format required by LINFLUX, write on UNIT 51
4	PRE	interpolate (calculate) mode shape values at each aero-grid point on both the airfoil surfaces for all modes (UNIT 27); out.mode.1; out.mode.2 .....out.mode.NM
5	LINFLUX	calculate unsteady pressures for the given mode, frequency and interblade phase angle; repeat for all modes, frequencies and interblade phase angles (UNIT 94); out.prss.1 and out.prsp.1; out.prss.2, out.prsp.2 .....out.prss.NM, out.prsp.NM
6	POST	calculate generalized forces; flutter eigenvalues and response

Table 2: Comparison of work/cycle, $\bar{\omega}$ = 0.7, Helical fan, M=0.5, Ω=16962 rpm

Plunging

sigma	ND	LINFLUX	TURBO-AE
0	0	-1.6854-02	-1.6907-02
90	6	-2.5382-02	-2.5351-02
180	12	-4.616-02	-4.5597-02
270	-6	-2.863-02	-3.5906-02

Pitching about mid-chord

sigma	ND	LINFLUX	TURBO-AE
0	0	-0.13928-03	-0.26938-03
90	6	-0.13334-03	-0.24221-03
180	12	-0.33714-03	-0.06438-02
270	-6	-0.35759-03	-0.07989-02

Table 3: Eigenvalue comparison, Helical fan

mode	LINFLUX-AE		ASTROP2	
	Eigenvalue		Eigenvalue	
	real	imaginary	real	imaginary
1	-0.6533-06	0.1527+04	-0.4637-06	0.152704+04
2	-0.1024-08	0.4500+04	-0.8846-08	0.45000+04

Table 4: Comparison of work/cycle, E-cubed fan, M=0.5, Ω= 2727 rpm

mode 1; $\bar{\omega}$ = 2.732

sigma	ND	LINFLUX	TURBO-AE
0	0	-0.18668-03	-0.7225-03
90	8	-0.87189-03	-0.3526-02
180	16	-0.2394-02	-0.6938-02
270	-8	-0.18337-02	-0.3836-02

mode 2; $\bar{\omega}$ = 4.183

sigma	ND	LINFLUX	TURBO-AE
0	0	-0.7853-03	-0.4225-02
90	8	*	0.2108-03
180	16	*	-0.5518-02
270	-8	-0.53142-03	-1.1175-02

* the solution did not converge;
got into numerically unstable region

Table 5: Eigenvalue comparison, E-cubed fan

mode	LINFLUX-AE		ASTROP2	
	Eigenvalue		Eigenvalue	
	real	imaginary	real	imaginary
1	-0.1001-00	0.7217+02	-0.5242+00	0.7191+02
2	-0.7807-01	0.1632+03	-0.3021+01	0.1635+03

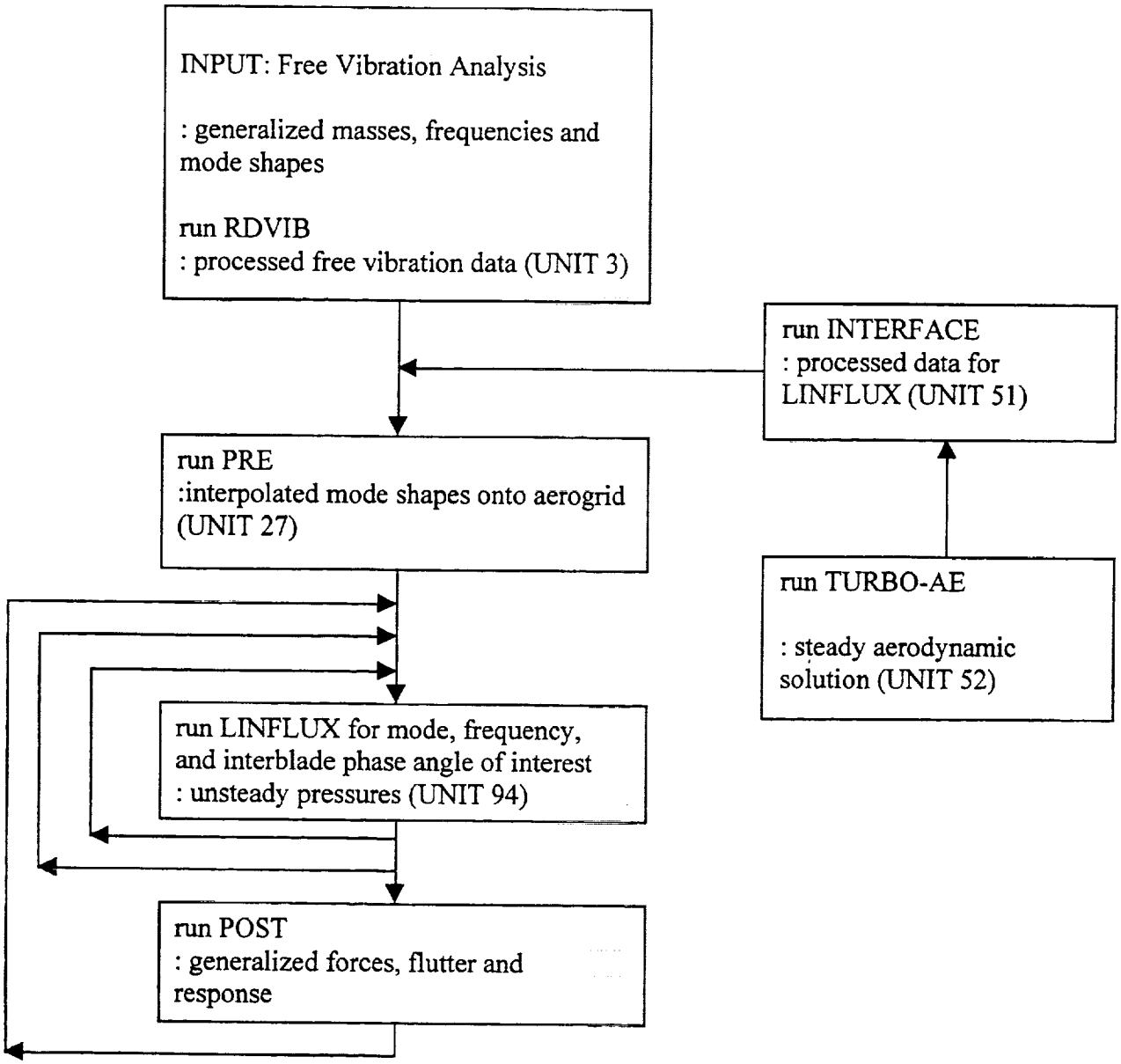

Figure 1 : LINFLUX-AE flow chart

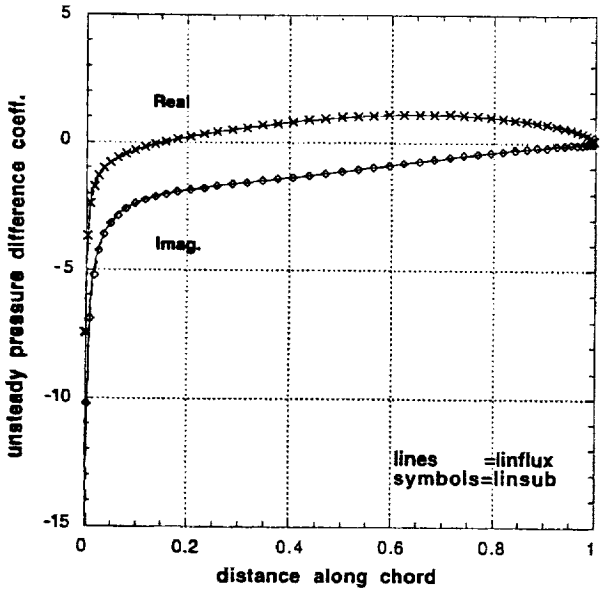

Figure 2.1 Unsteady pressures for plunging motion, $\sigma = 0°$, helical fan, $\overline{\omega} = 0.7$, Mr=0.7

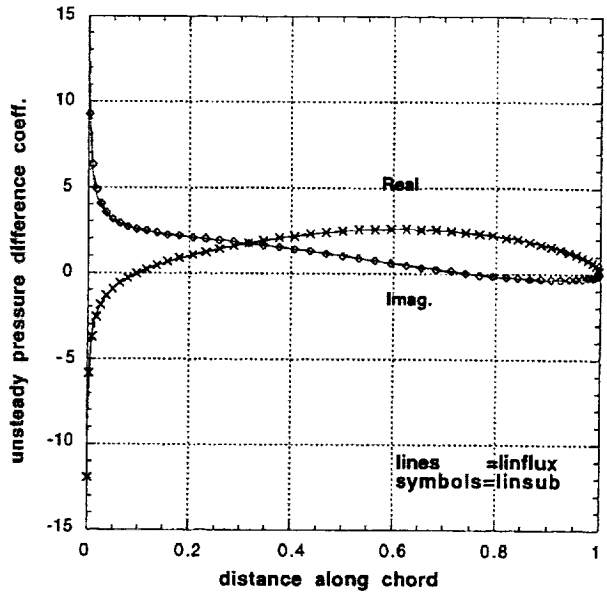

Figure 3.1 Unsteady pressure distribution for pitching about leading edge, $\sigma = 0°$, helical fan, $\overline{\omega} = 0.7$, Mr=0.7

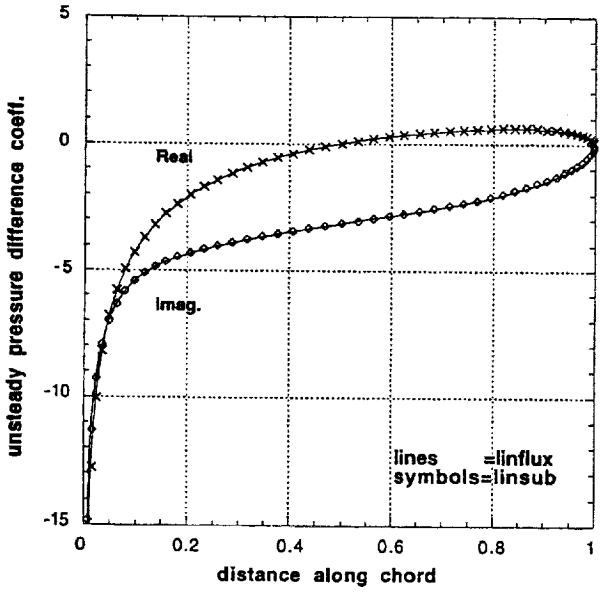

Figure 2.2 Unsteady pressures for plunging motion, $\sigma = 180°$, helical fan, $\overline{\omega} = 0.7$, Mr=0.7

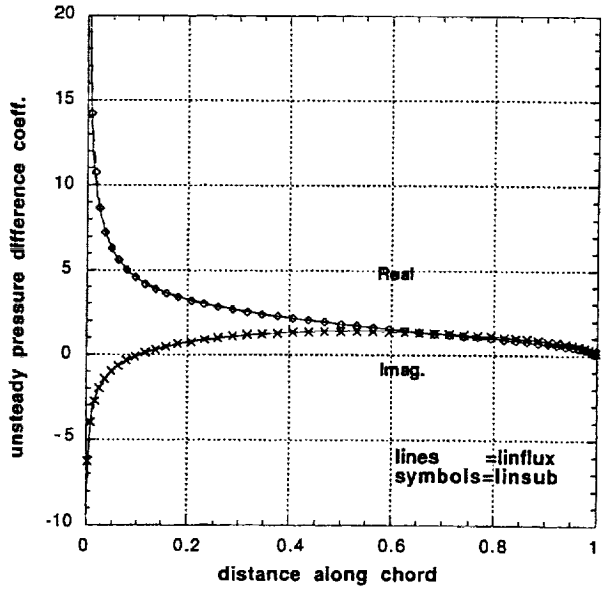

Figure 3.2 Unsteady pressure distribution for pitching about leading edge, $\sigma = 90°$, helical fan, $\overline{\omega} = 0.7$, Mr=0.7

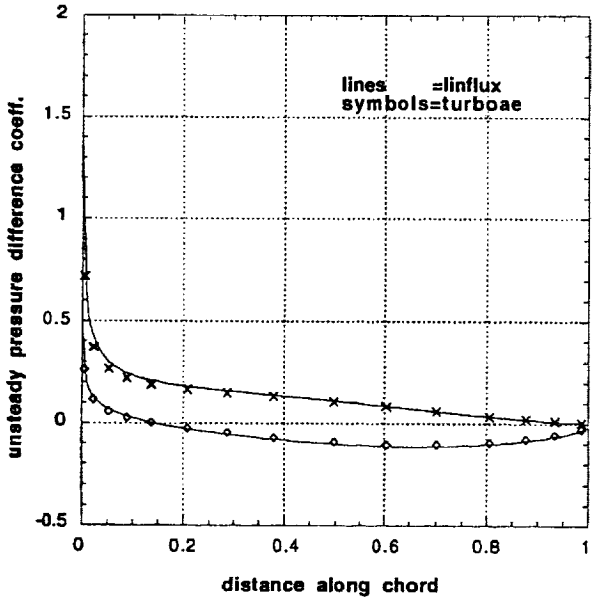

Figure 4.1 Unsteady pressure comparison, helical fan, LINFLUX vs TURBO-AE, plunging, $\sigma = 0°$.

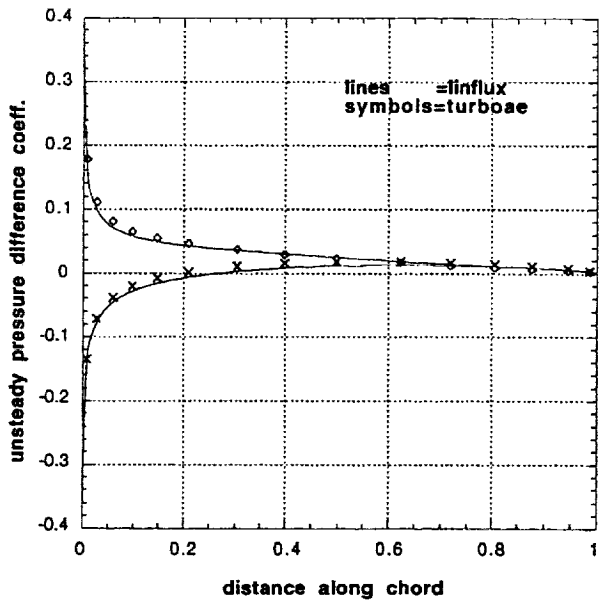

Figure 5.1 Unsteady pressures, pitching about mid-chord, helical fan, LINFLUX vs TURBO-AE, $\sigma = 0°$

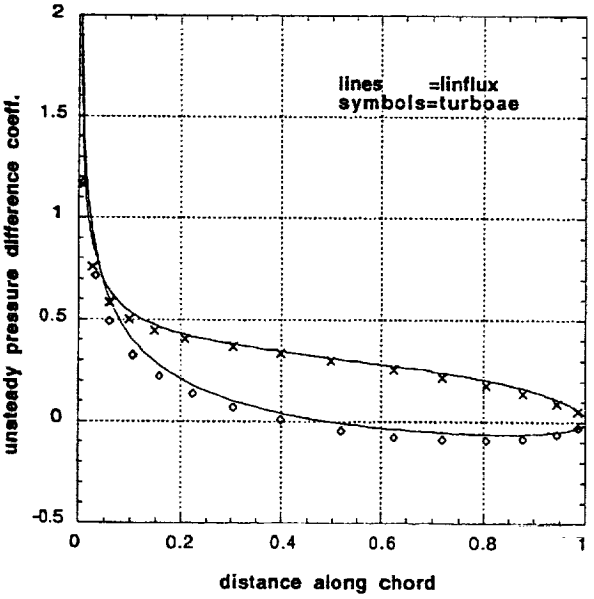

Figure 4.2 Unsteady pressure, helical fan, sigma=180, LINFLUX vs TURBO-AE, $\sigma = 180°$

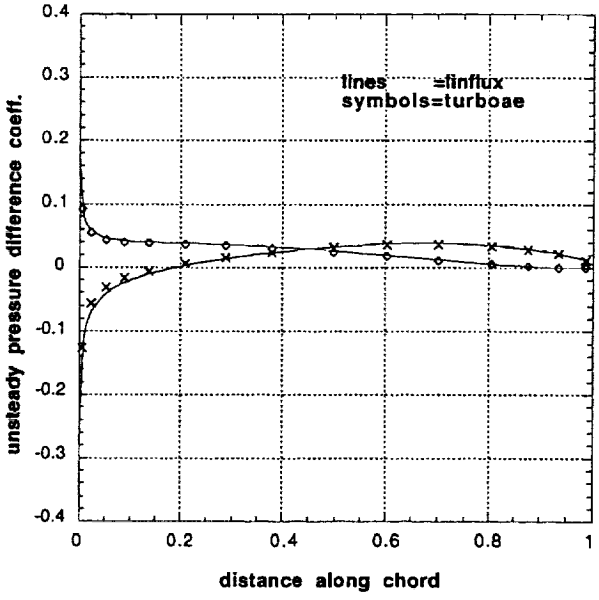

Figure 5.2 Unsteady pressures, LINFLUX vs TURBO-AE, helical fan, $\sigma = 90°$, pitching about mid-chord

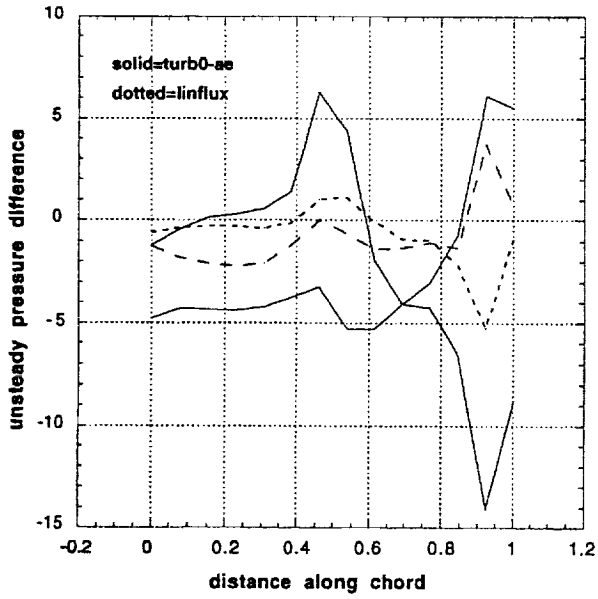

Figure 7.1 Unsteady pressure distribution for mode 2, E-cubed fan, $\overline{\omega} = 4.183$, $\sigma = 0°$.

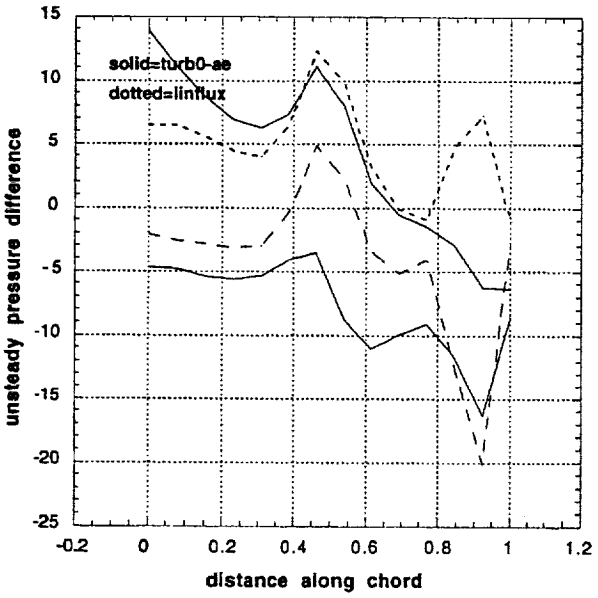

Figure 7.2 Unsteady pressure distribution for mode 2, E-cubed fan, $\overline{\omega} = 4.183$, $\sigma = 270°$